Homogeneous CO Hydrogenation: Dihydrogen Activation Involves a Frustrated Lewis Pair Instead of a Platinum Complex

Alexander J. M. Miller, Jay A. Labinger,* and John E. Bercaw*

Arnold and Mabel Beckman Laboratories of Chemical Synthesis, California Institute of Technology, Pasadena, California 91125

Supporting Information

Table of Contents **Page**

List of Figures **Page**

I. Experimental Section

i. General Considerations.

All air- and moisture-sensitive compounds were manipulated using standard vacuum line or Schlenk techniques, or in a glovebox under a nitrogen atmosphere. NMR scale reactions involving J-Young NMR tubes were set up in an intert atmosphere glovebox, unless otherwise specified. Under standard glovebox conditions, petroleum ether, diethyl ether, benzene, toluene, and tetrahydrofuran were used without purging, such that traces of those solvents were in the atmosphere, and could be found intermixed in the solvent bottles. The solvents for air- and moisture-sensitive reactions were dried over sodium benzophenone ketyl, calcium hydride, or by the method of Grubbs.[1] All NMR solvents were purchased from Cambridge Isotopes Laboratories, Inc. Chlorobenzene-d_5 (C_6D_5Cl) and dichloromethane-d_2 (CD_2Cl_2) were freeze-pump-thaw degassed three times before being run through a small column of activated alumina. Tetrahydrofuran-d_8 (THF-d_8) was purchased in a sealed ampoule, and dried by passage through activated alumina. Unless noted, other materials were used as received. [**1**][BF_4][2] and [$(PPh_3)_2Re(CO)_4$][BF_4][3] were prepared according to literature procedures; treatment with 1 equiv $NaBAr^F_4$ in CH_2Cl_2 afforded anion exchange to yield [**1**][BAr^F_4] and [$(PPh_3)_2Re(CO)_4$][BAr^F_4] essentially quantitatively, after filtration and removal of solvents. [$Pt(dmpe)_2$][PF_6]$_2$,[3] [$HPt(dmpe)_2$][PF_6],[3] [$Ni(dmpe)_2$][BF_4]$_2$,[4] [$HNi(dmpe)_2$][PF_6],[3] ^{t}BuCH$_2$CH$_2$B(C_8H_{14}),[5] and KOPh[6] were synthesized by literature methods. *tert*-Butylimino-tris(dimethylamino)phosphorane (**P$_1$**) was purchased from Sigma-Aldrich. All other materials were readily commercially available, and used as received. ^{1}H and ^{13}C NMR spectra were recorded on Varian Mercury 300 MHz, or Varian INOVA-500 or 600 MHz spectrometers at room temperature, unless indicated otherwise. Chemical shifts are reported with respect to residual internal protio solvent for ^{1}H and ^{13}C{^{1}H} spectra. Other nuclei were referenced to an external standard: H_3PO_4 (^{31}P), 15% BF_3•Et_2O/$CDCl_3$ (^{11}B), $CFCl_3$ (^{19}F), all at 0 ppm.

ii. X-ray Crystallography Procedures.

Colorless single crystals of [**1**•$(THF)_2$][BF_4] suitable for X-Ray diffraction were grown by vapor diffusion of pentane into a THF solution of [**1**][BF_4]. The crystals were mounted on a glass fiber with Paratone-N oil. Structures were determined using direct methods with standard Fourier techniques using the Bruker AXS software package. In some cases, Patterson maps were used in place of the direct methods procedure. There was some disorder in the BF_4 group, as discussed in the crystallographic details section, but connectivity was unambiguously established as a bis-THF adduct.

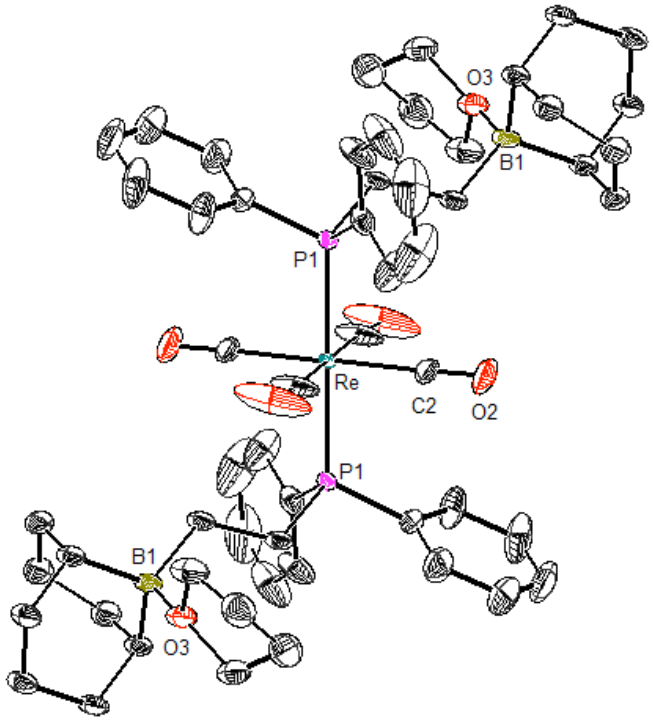

Figure S1. Structural representation of [**1**•$(THF)_2$][BF_4] (ellipsoids at 50% probability), with BF_4 group and hydrogen atoms omitted for clarity. Selected bond distances (Å): Re-C1 1.983(1), Re-C2 1.990(1), Re-P1 2.4324(2), O1-C1 1.127(2), O2-C2 1.135(2), O3-B1 1.683(2).

iii. Adduct formation between THF and [1][BF_4].

In a glovebox, a J-Young Teflon-stoppered NMR tube was charged with 43.9 mg (0.0417 mmol) [**1**][BF_4] and ~0.6 mL CD_2Cl_2. Initial ^1H and ^{11}B NMR spectra were recorded. The tube was returned to the glove box, and 3.4 μL (0.0417 mmol, 1 equiv) THF was added by syringe. After collecting ^1H and ^{11}B NMR spectra, the procedure was repeated, adding THF to give 3, 5, 9, 13, 17, 25, and 33 equivalents relative to $[\mathbf{1}]^+$.

A Benesi-Hildebrand-type analysis[7,8] was performed according to a previously described derivation.[9] The THF dependence on chemical shift of the ^{11}B resonance and several ^1H resonances were recorded, and a Benesi-Hildebrand plot of 1/[THF] vs. 1/Δδ was obtained (Fig. S2), where Δδ is the change in chemical shift between each addition of THF. The very broad ^{11}B resonance gave a satisfactory fit, but the CH_2 resonances in the ^1H NMR fit Benesi-Hildebrand relation better. The slope = $1/[(\Delta\delta)(K_{eq})]$, allowing K_{eq} for formation of the adduct with one of the pendant borane arms to be calculated. K_{eq} = 0.19(2) M^{-1} (average of three ^1H resonances).

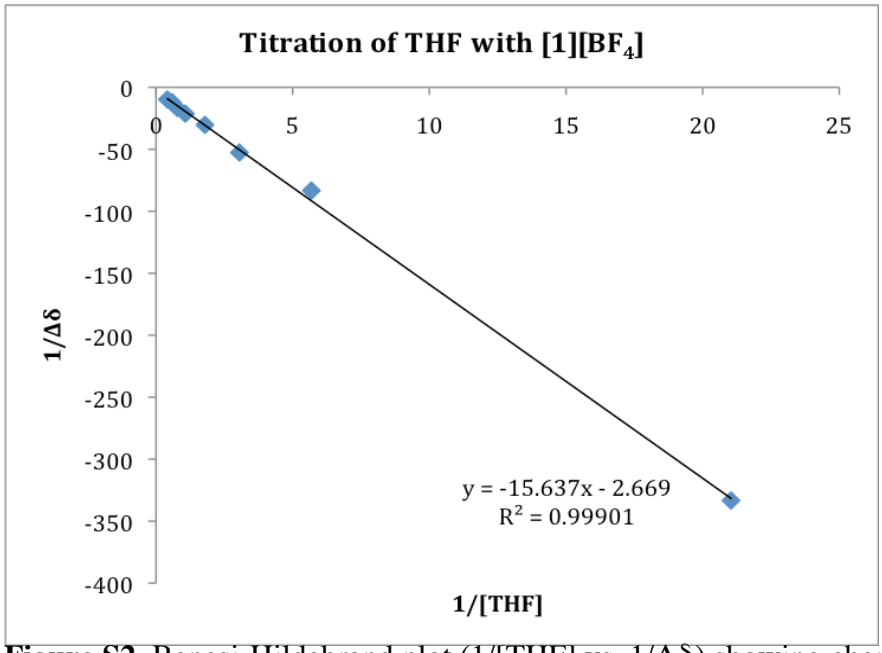

Figure S2. Benesi-Hildebrand plot (1/[THF] vs. 1/Δδ) showing chemical shift dependence on added THF.

iv. Synthetic Procedures and Reactions:

Preparation of $[Pt(dmpe)_2][BAr^F{}_4]_2$.

The procedure for the preparation of $[Pt(dmpe)_2][PF_6]_2$ was followed,[3] except that the intermediate $[Pt(dmpe)_2][Cl]_2$ was treated with $NaBAr^F{}_4$ rather than $[NH_4][PF_6]$. In a glovebox, a 100 mL round bottom flask was charged with 1.0 g (2.7 mmol) $Pt(COD)(Cl)_2$, 0.8 g (5.3 mmol) 1,2-bis(dimethylphosphino)ethane, and 30 mL acetonitrile. The reaction mixture was stirred overnight. After ~12 hours, the acetonitrile was removed *in vacuo*, and the solids were dissolved in 40 mL of water under air. To the colorless solution was added 4.7 g (5.3 mmol) $NaBAr^F{}_4$ as a solid, and the slurry was stirred for ~24 hours. The white solids were collected by filtration through a sintered glass frit, washed with 70 mL CH_2Cl_2, and dried *in vacuo* to afford 1.2 g (0.5 mmol, 25%) $[Pt(dmpe)_2][BAr^F{}_4]_2$. The product was spectroscopically very similar to $[Pt(dmpe)_2][PF_6]_2$.[3] ^{1}H NMR (THF-d_8, 300 MHz): δ 1.96 (m, $^3J_{PtH}$ = 27.7 Hz, 24H, $Me_2PCH_2CH_2PMe_2$), 2.30 (m, 8H, $Me_2PCH_2CH_2PMe_2$), 7.59 (8H, $BAr^F{}_4$), 7.80 (16H, $BAr^F{}_4$). ^{31}P{^{1}H} NMR (THF-d_8, 121 MHz): δ 33.6 (s, $^1J_{PtP}$ = 2109 Hz).

Preparation of $[HPt(dmpe)_2][BAr^F{}_4]$.

To a stirring 10 mL CH_2Cl_2 solution of 102.8 mg (0.16 mmol) $[HPt(dmpe)_2][PF_6]$ was added solid $NaBAr^F{}_4$ (142.1 mg, 0.16 mmol). The suspension was stirred for 6 hours, then filtered through celite, washing with 2 mL CH_2Cl_2. The filtrate was dried *in vacuo*, affording 194 mg (0.14 mmol, 89%) spectroscopically pure $[HPt(dmpe)_2][BAr^F{}_4]$. The product was spectroscopically very similar to $[HPt(dmpe)_2][PF_6]$.[3] ^{1}H NMR (C_6D_5Cl, 300 MHz): δ -11.94 (p, $^2J_{PH}$ = 29.8 Hz, $^1J_{PtH}$ = 700.9 Hz, 1H, *H*Pt), 1.16 (m, $^3J_{PtH}$ = 22.7 Hz, 24H, $Me_2PCH_2CH_2PMe_2$), 1.22 (m, 8H, $Me_2PCH_2CH_2PMe_2$), 7.61 (4H, $BAr^F{}_4$), 8.23 (m,

8H, BAr^F_4). $^{31}P\{^1H\}$ NMR (C_6D_5Cl, 121 MHz): δ -8.0 (s, J_{PtP} = 2234 Hz). ^{19}F NMR (C_6D_5Cl, 282 MHz): δ -62.3.

Preparation of $[Ni(dmpe)_2][BAr^F_4]_2$.
A slurry of 358 mg (0.358 mmol) $[Ni(dmpe)_2][BF_4]_2$ in 10 mL CH_2Cl_2 was treated with 635 mg (0.717, 2 equiv) solid $NaBAr^F_4$. The mixture was stirred ~12 hours, then filtered, giving a yellow filtrate with plenty of light yellow solids remaining on the fritted funnel. The filtrate was dried under vacuum, giving a low (20%) yield of pure $[Ni(dmpe)_2][BAr^F_4]_2$, which was identified by comparison of NMR resonances to the previously reported $[BF_4]$ salt.[4] ^1H NMR (THF-d_8, 300 MHz): δ 1.82 (m, 24 H, $Me_2PCH_2CH_2PMe_2$), 2.29 (m, 8H, $Me_2PCH_2CH_2PMe_2$), 7.58 (8H, BAr^F_4), 7.79 (m, 16H, BAr^F_4). $^{31}P\{^1H\}$ NMR (THF-d_8, 121 MHz): δ 45.3. ^{19}F NMR (THF-d_8, 282 MHz): δ -66.

NMR Scale Reaction of KOPh with $[1][BF_4]$, and subsequent attempted reduction with $[HPt]^+$.
A J-Young NMR tube was charged with 22.4 mg (0.021 mmol) [**1**][BF_4], 11.3 mg (0.085 mmol) KOPh, and ~0.6 mL THF-d_8. Some fine precipitates were visible, although the bulk of the KOPh (mostly insoluble in THF) seemed to dissolve. NMR analysis after 20 minutes revealed complete conversion to a new symmetric species (^{31}P δ 2.1). IR spectroscopy (THF solution) showed a single CO stretch at 1990 cm^{-1} (s), shifted slightly from 1998 cm^{-1} in [**1**][BF_4], consistent with a tetracarbonyl structure (PhO^- stretches were observed at 1585 and 1490 cm^{-1}). ^{11}B NMR showed a broad resonance at δ -0.1, but neither a downfield resonances consistent with 3-coordinate boron, nor a $[BF_4]^-$ resonance was observed. Taken together, these data are consistent with phenoxide addition to the borane of $[\mathbf{1}]^+$ to give a zwitterionic borate species, which would be anionic (accounting for the slight IR shift to lower energy). There is no IR or NMR evidence of attack at a carbonyl. Nonetheless, addition of 14 mg (0.022 mmol) [**HPt**][PF_6] to this mixture resulted in no detectable reaction, confirming that no Lewis acid-assisted reduction takes place.

NMR scale reaction of $[1][BF_4]$ with $[HPt][PF_6]$ in THF-d_8.
A small vial was charged with 30 mg (0.029 mmol) [**1**][BF_4] and ~0.6 mL THF-d_8. With stirring, 18 mg (0.029 mmol) [**HPt**][PF_6] was added as a solid, portionwise. The mixture, containing some precipitates, was transferred to an NMR tube, and NMR spectra showed partial conversion (~50%) to a formyl species, which disproportionated overnight to give $[\mathbf{3}]^-$ and $[\mathbf{1}]^+$. The viability of THF as a solvent medium for Lewis-acid assisted reductions was thus established.

NMR scale reaction of $[1][BF_4]$ with pyridine, and attempted reaction with $[HPt][PF_6]$.
A J-Young NMR tube was charged with 27.7 mg (0.026 mmol) [**1**][BF_4] and ~0.6 mL C_6D_5Cl. Pyridine (4.2 μL, 0.052 mmol, 2 equiv) was added by syringe, and the tube was sealed. Multinuclear NMR spectroscopy was consistent with strong adduct formation: a new set of pyridine resonances, distinct from free pyridine, was observed by ^1H NMR; the CH_2 protons of $[\mathbf{1}]^+$ shifted upfield by ~1 ppm; the ^{31}P resonance of $[\mathbf{1}]^+$ shifted slightly (δ 2.1, vs. δ 1.3 for pure [**1**][BF_4] in C_6D_5Cl); and the ^{11}B resonance of $[\mathbf{1}]^+$

shifted upfield. The resonance was far enough upfield to be obstructed by the large borosilicate signal due to glass construction in the probe. The tube was returned to the glovebox, and the reaction mixture was poured onto 16.6 mg (0.026 mmol, 1 equiv) solid [**HPt**][PF_6]. The solution was returned to the tube, and monitored by NMR. No reduction to **2** or [**3**]$^-$ was observed, nor was any consumption of [**HPt**][PF_6] seen after 24 hours. ^{1}H NMR (C_6D_5Cl, 500 MHz) of pyridine adduct: δ 0.42 (br s, 2H, $Ph_2PCH_2CH_2B(C_8H_{14})$), 1.00 (br s, 2H -$B(C_8H_{14})$), 1.3 (m, 3H, -$B(C_8H_{14})$), 1.47 (m, 1H, -$B(C_8H_{14})$), 1.6 (m, 4H, -$B(C_8H_{14})$), 1.79 (m, 2H, -$B(C_8H_{14})$), 1.90 (m, 2H, -$B(C_8H_{14})$), 2.26 (br m, 2H, $Ph_2PCH_2CH_2B(C_8H_{14})$), 7.17 (t, J = 7.3 Hz, 2H, pyridine), 7.25 (t, J = 7.46, 4H, $Ph_2PCH_2CH_2B(C_8H_{14})$), 7.38 (m, 6H, $Ph_2PCH_2CH_2B(C_8H_{14})$), 7.67 (t, J = 7.4 Hz, 1H, pyridine), 8.25 (d, J = 5.5 Hz, 2H, pyridine). ^{11}B NMR (C_6D_5Cl, 500 MHz): δ 0.0 ([BF_4]$^-$). ^{31}P{^{1}H} NMR (C_6D_5Cl, 121 MHz): δ 2.1.

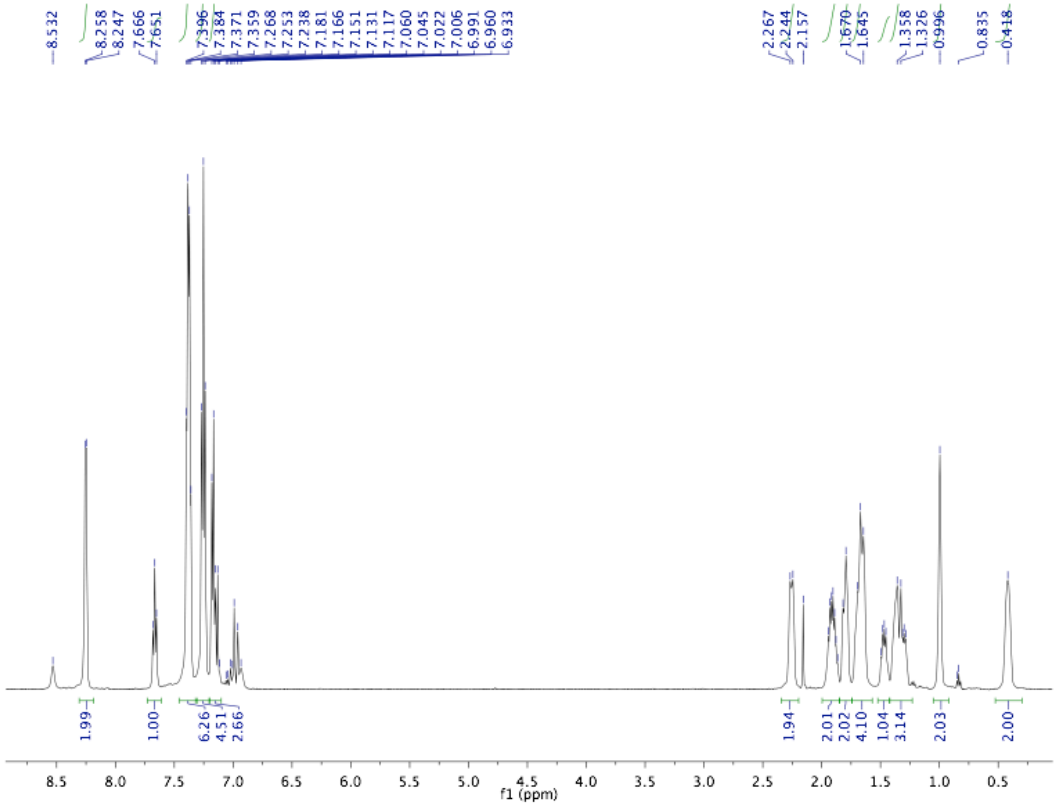

Figure S3. ^{1}H NMR after pyridine addition.

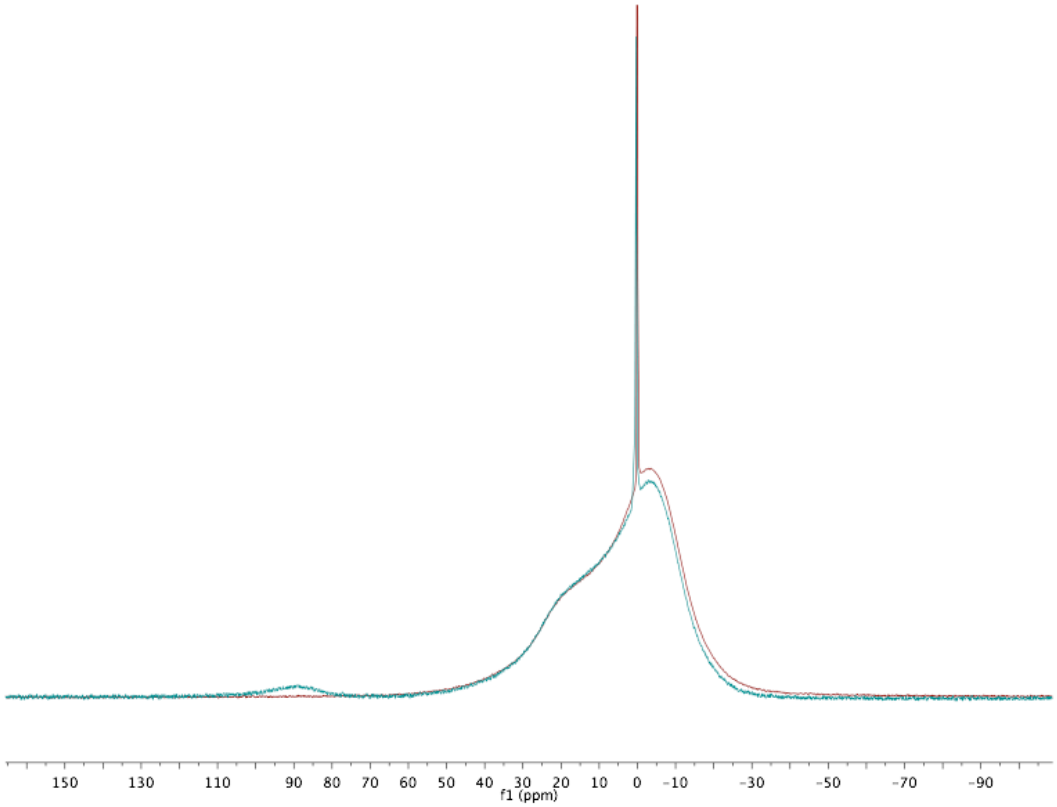

Figure S4. ^{11}B NMR after pyridine addition (red trace), compared with pure [**1**]$^+$ (blue trace).

Addition of NEt_3 to [1][BF_4]; Reduction of [1][BF_4] by [HPt][PF_6] in the presence of NEt_3.

Two separate experiments were carried out. First, [**1**][BF_4] and NEt_3 were mixed to determine whether strong adduct formation would occur. A J-Young NMR tube was charged with 25.5 mg (0.024 mmol) [**1**][BF_4], 4.9 mg (0.048 mmol, 2 equiv) NEt_3, and ~0.6 mL CD_2Cl_2. The tube was sealed and ^{1}H, ^{11}B, and ^{31}P{^{1}H} NMR were acquired, showing minimal interaction between NEt_3 and [**1**]$^+$.

Next, reduction was attempted in the presence of NEt_3. A small vial was charged with 23.4 mg (0.022 mmol) [**1**][BF_4] and ~0.6 mL THF-d_8. NEt_3 (6.2 µL, 0.044 mmol, 2 equiv) was added by syringe, and the mixture was stirred for 1 minute, after which time solid [**HPt**][PF_6] (31 mg, 0.048 mmol, 2.2 equiv) was added. The colorless solution quickly turned bright yellow. The reaction mixture was transferred to an NMR tube, and ^{1}H and ^{31}P NMR spectra revealed complete conversion of [**1**]$^+$ to [**3**]$^-$, along with some unreacted [**HPt**]$^+$ (as an excess was present).

Addition of P_1 to [1][BF_4]; Reduction of [1][BF_4] by [HPt][PF_6] in the presence of P_1.

Two separate experiments were carried out. First, the stability of [**1**][BF_4] to **P_1** was established. In a glovebox, 20.2 mg (0.019 mmol) [**1**][BF_4], 6.0 mg (0.019 mmol) **P_1**, and ~0.6 mL C_6D_5Cl were combined in a J-Young NMR tube. The tube was sealed, and the reaction monitored over a few days. Shifts were observed in some resonances of the ^{1}H NMR spectrum (see overlay in Figure S5); a shift was also observed in the ^{11}B NMR

spectrum, to δ 82.7 (from δ 87.7 in pure [**1**][BF_4], but still ~80 ppm from normal 4-coordinate region.); only a very minor shift was noted in the $^{31}P\{^1H\}$ NMR, to δ 1.7 (pure [**1**][BF_4], δ 1.3 in C_6D_5Cl). The lack of broadening indicates that any interaction is fast and reversible on the NMR timescale, and the minor shifts indicate that the equilibrium lies towards no interaction. Very minor (1-2%) degradation was observed over 2 days.

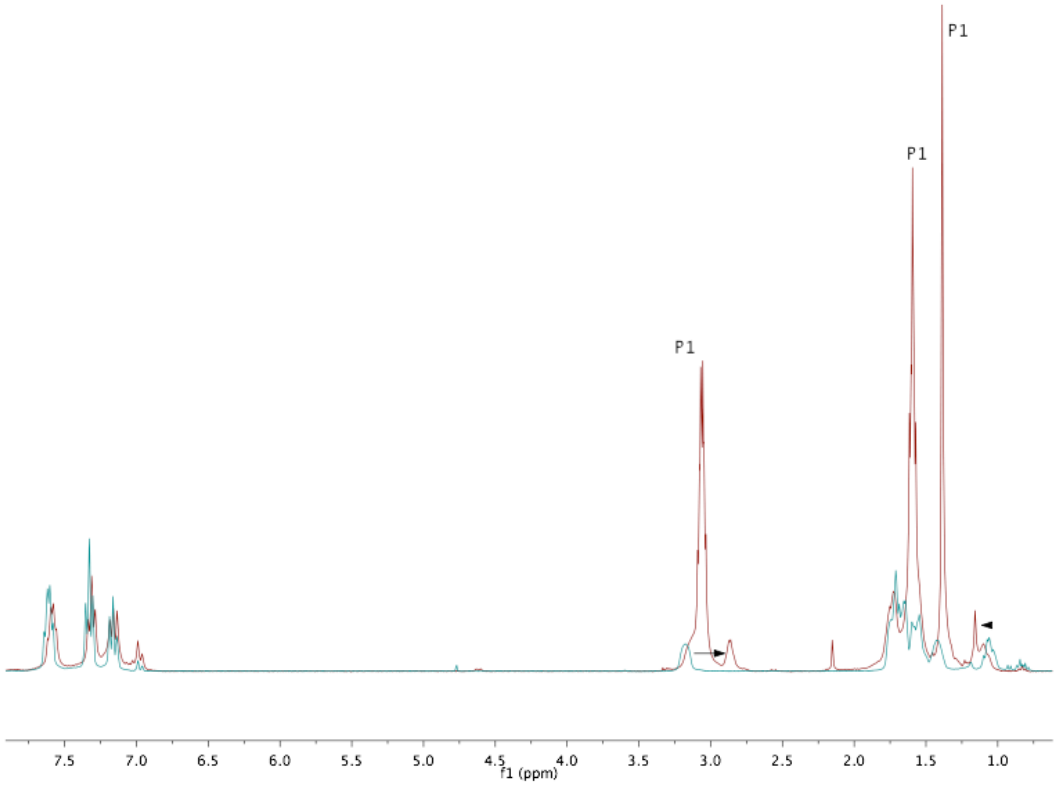

Figure S5. ^1H NMR of [**1**][BF_4] in the presence of $\mathbf{P_1}$ (red trace), overlaid with pure [**1**][BF_4] (blue).

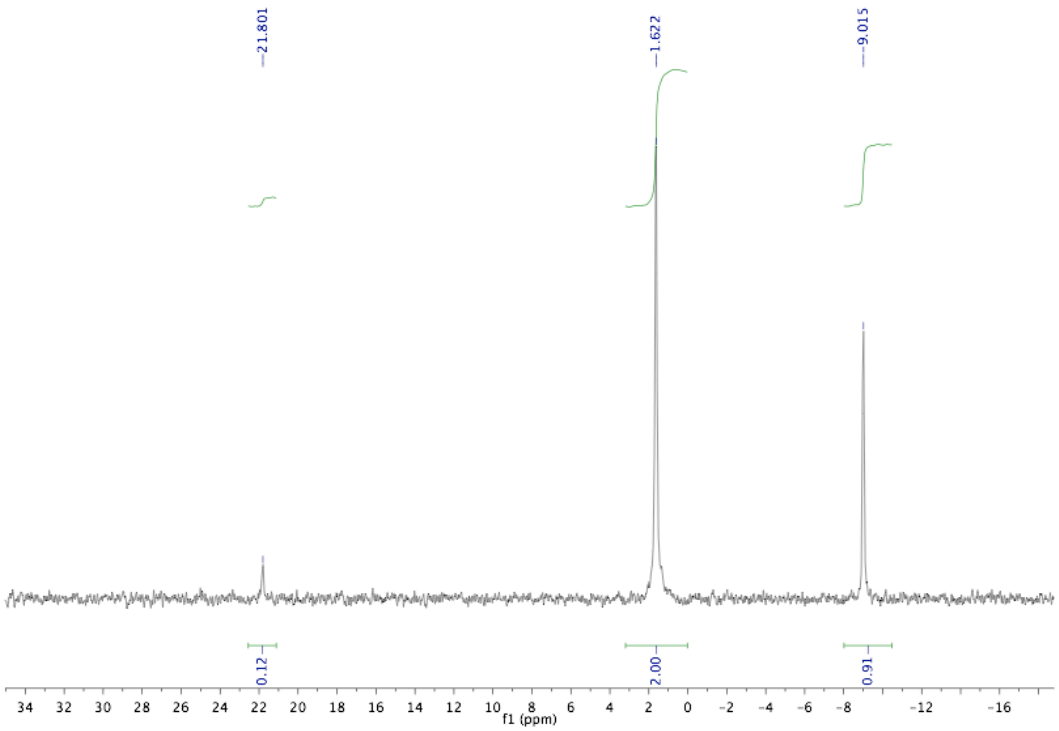

Figure S6. $^{31}P\{^{1}H\}$ NMR of [**1**][BF_4] in the presence of $\mathbf{P_1}$ (peak at 21.8 is small amount of $[\mathbf{HP_1}]^+$)

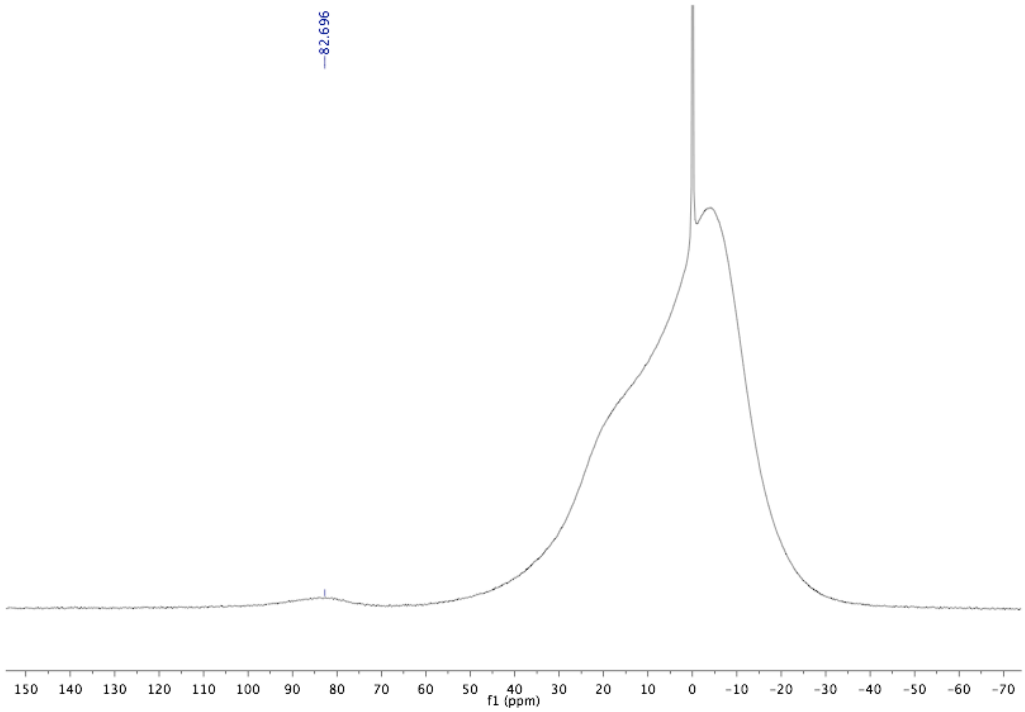

Figure S7. ^{11}B NMR of [**1**][BF_4] in the presence of $\mathbf{P_1}$ (sharp peak is $[BF_4]^-$).

To establish whether $[\mathbf{1}]^+$ could be reduced by $[\mathbf{HPt}]^+$ in the presence of $\mathbf{P_1}$, a J-Young NMR tube was charged with 27.3 mg (0.026 mmol) $[\mathbf{1}]^+$, 8.1 mg (0.026 mmol) $\mathbf{P_1}$, 16.6

mg (0.026 mmol) [**HPt**]$^+$, and ~0.6 mL THF-d_8. The tube was sealed and shaken to mix. The solution turned yellow, and after 30 minutes, the major product was **2**, along with [**3**]$^-$ and unreacted [**1**]$^+$ ([**1**]$^+$:**2**:[**3**]$^-$ of 1.0:3.2:1.2). Essentially all [**HPt**]$^+$ had reacted already. After 4 hours, **2** had mostly disproportionated to [**3**]$^-$ and [**1**]$^+$ ([**1**]$^+$:**2**:[**3**]$^-$ of 1.0:0.3:1.2).

Heterolytic cleavage of H_2 with [Pt][BAr$^F{}_4$]$_2$ and P_1.
A J-Young Teflon-sealed NMR tube was charged with 16.4 mg (0.0074 mmol) [**Pt**][BAr$^F{}_4$]$_2$, 23.1 mg (0.074 mmol, 10 equiv) $\mathbf{P_1}$, and ~0.6 mL THF-d_8. The tube was degassed by two freeze-pump-thaw cycles, and ~3 atm H_2 (~0.2 mmol, ~30 equiv) was condensed into the tube at 77 K. The tube was sealed, carefully thawed, and monitored by ^{1}H and ^{31}P NMR. Clean first order transformation of [**Pt**][BAr$^F{}_4$]$_2$ into [**HPt**][BAr$^F{}_4$] was observed, along with formation of [$\mathbf{HP_1}$][BAr$^F{}_4$]. The phosphazene ^{31}P NMR signal broadened during the course of the reaction, presumably due to exchange with the generated [$\mathbf{HP_1}$]$^+$ (not observed). The half-life for the reaction was found to be 10.2 hours.

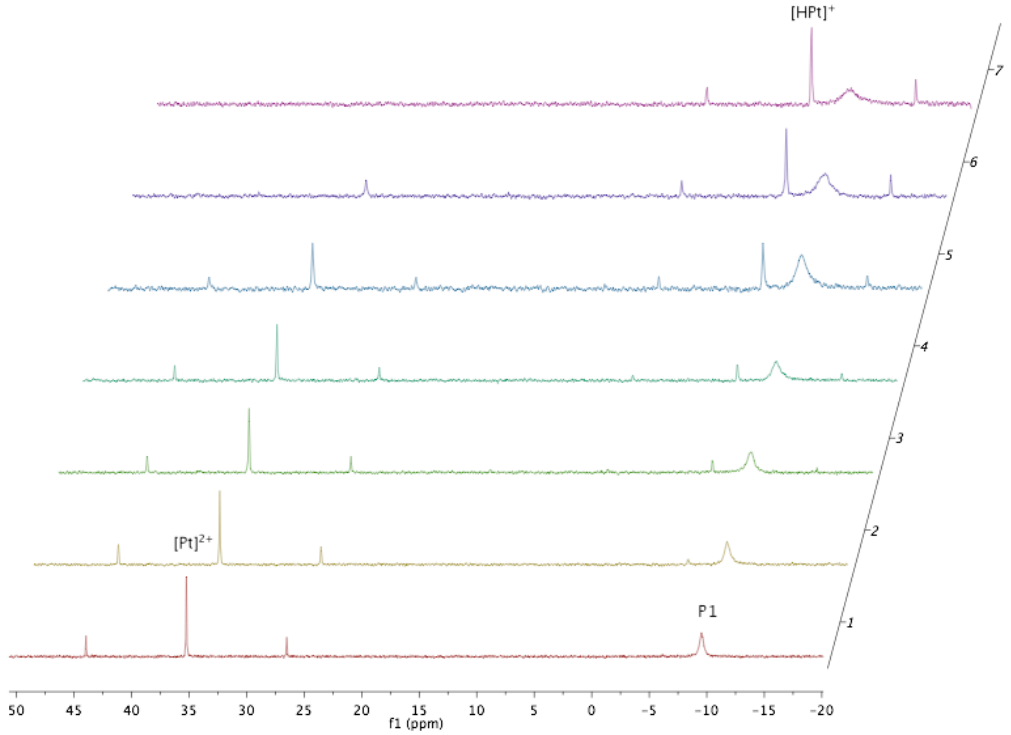

Figure S8. ^{31}P{^{1}H} NMR time course of H_2 splitting reaction.

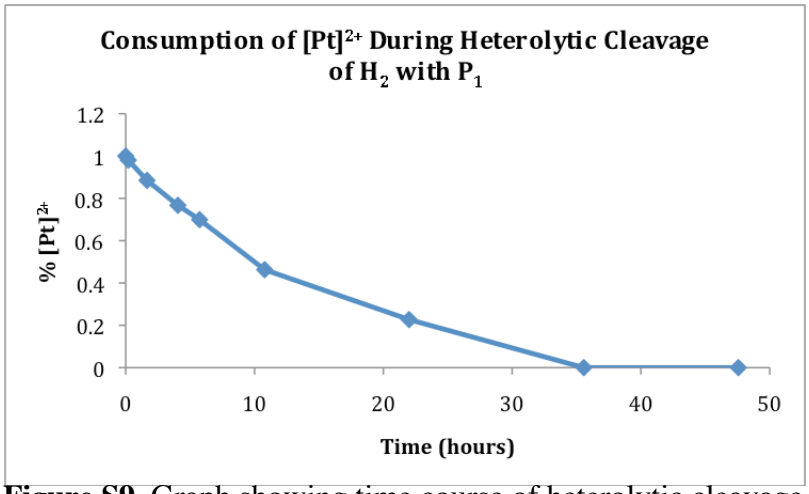

Figure S9. Graph showing time course of heterolytic cleavage reaction.

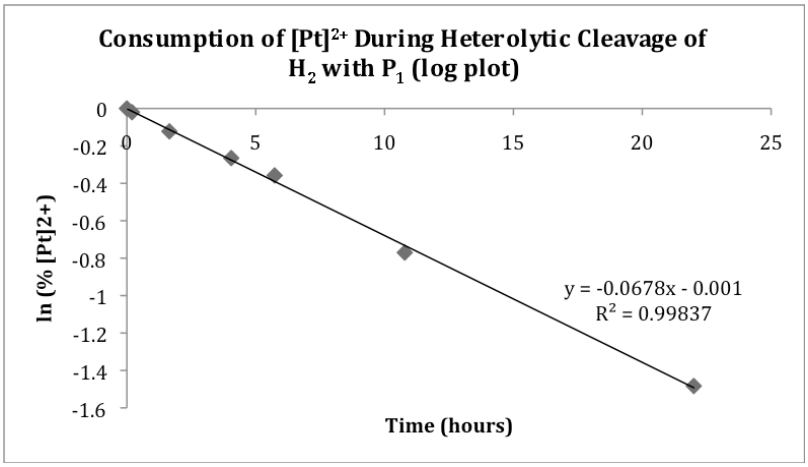

Figure S10. Graph showing log plot of time course of heterolytic cleavage reaction.

General Procedure for Metal-Added H_2 Reductions.
In a glovebox, a J-Young style Teflon-sealed NMR tube was charged with ~0.03 mmol [**1**][X] (X = BF_4 or BAr^F_4), ~0.06-0.60 mmol (2-20 equiv) $\mathbf{P_1}$, ~0.003-0.015 (0.1-0.5 equiv) $[M(dmpe)_2]^{2+}$ (M = Ni, Pt), and ~0.6 mL THF-d_8. The tube was sealed, and NMR spectra (^1H, $^{31}P\{^1H\}$) were obtained. The tube was degassed by two freeze-pump-thaw cycles, and between 1 and 4 atm H_2 was added by introducing an atmosphere of H_2 at either 298 or 77 K. The tube was affixed to a slowly spinning motor to ensure good mixing, and the reaction was monitored periodically by ^1H and ^{31}P NMR. Precise yields were measured by integration to a solution of $P(Mes)_3$ (Mes = 2,4,6-trimethylphenyl) in THF-d_8 in the J-Young tube in a coaxial capillary, with a range from 85-95% depending on conditions.

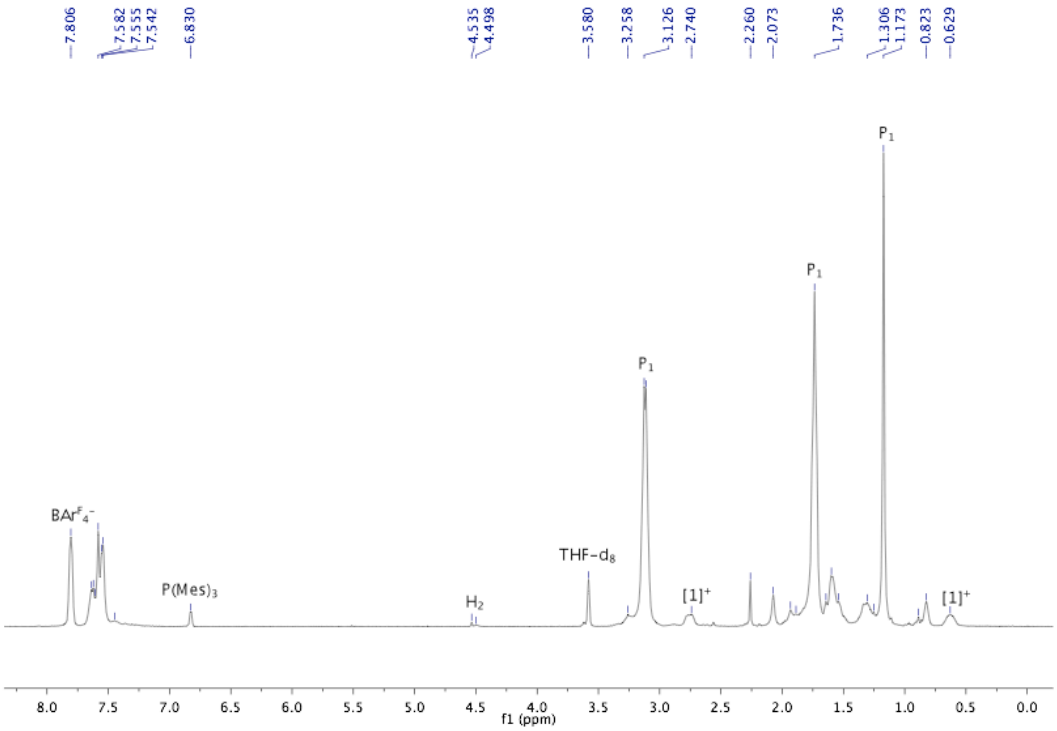

Figure S11. ^{1}H NMR immediately after H_2 addition (15 mol% $[\mathbf{Pt}]^{2+}$, 4 equiv $\mathbf{P_1}$).

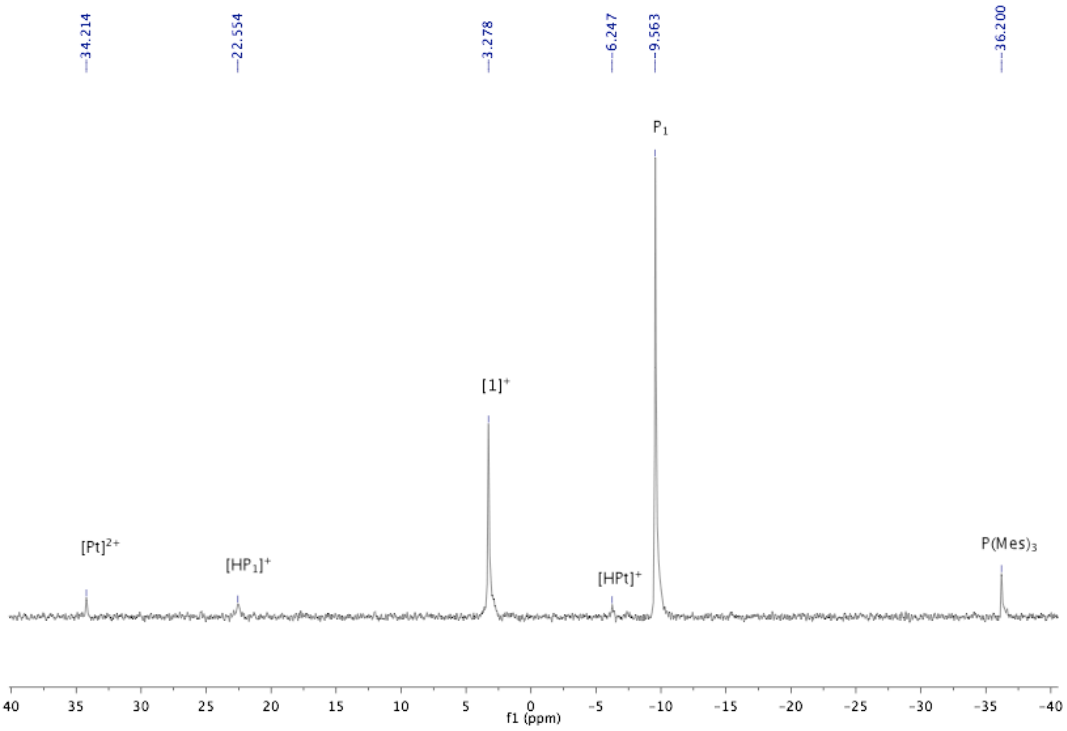

Figure S12. $^{31}P\{^{1}H\}$ NMR immediately after H_2 addition.

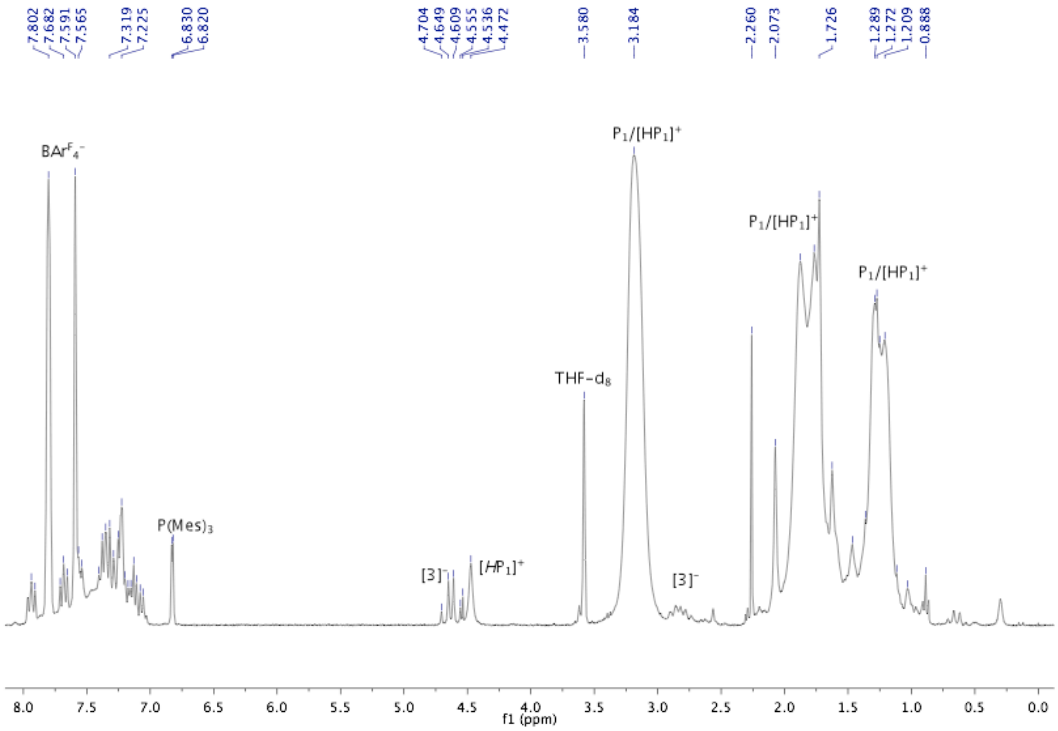

Figure S13. ^{1}H NMR after 13 days (reaction complete, 85% yield by integration).

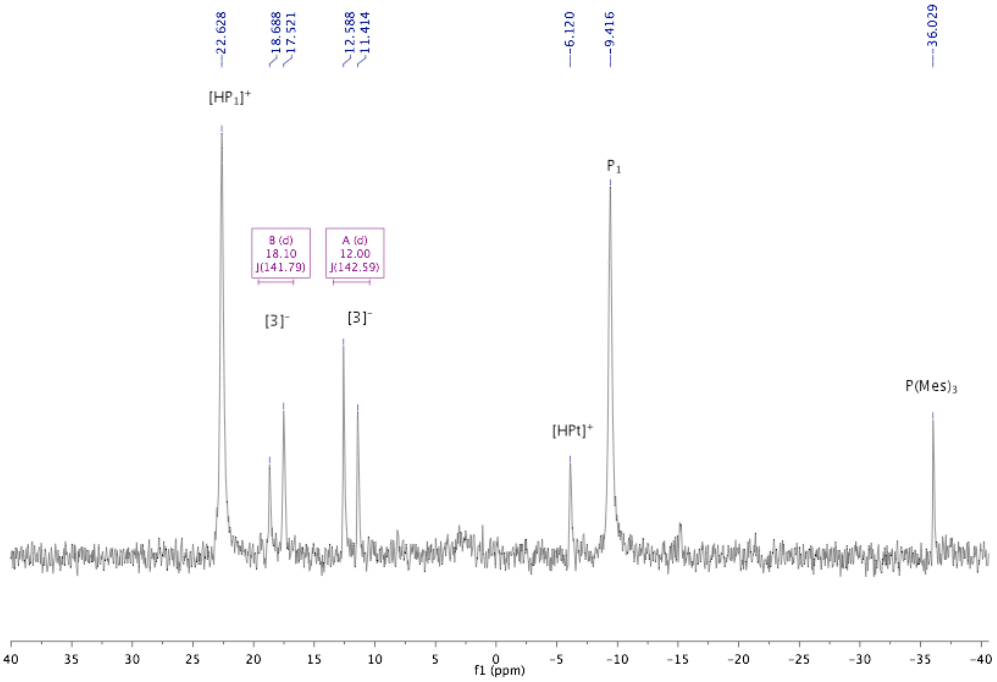

Figure S14. ^{31}P{^{1}H} NMR after 13 days.

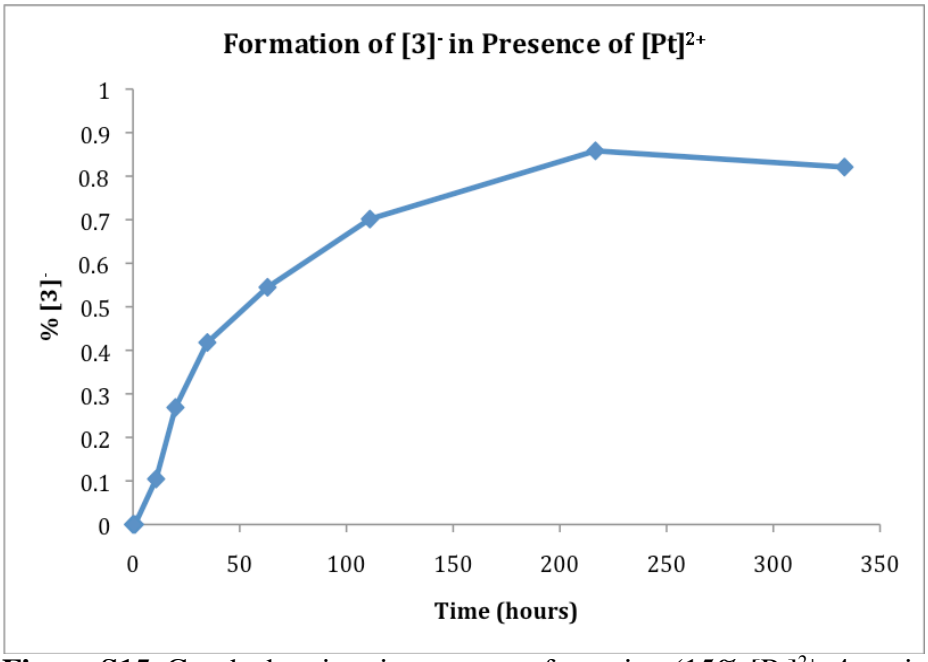

Figure S15. Graph showing time course of reaction (15% $[Pt]^{2+}$, 4 equiv H_2).

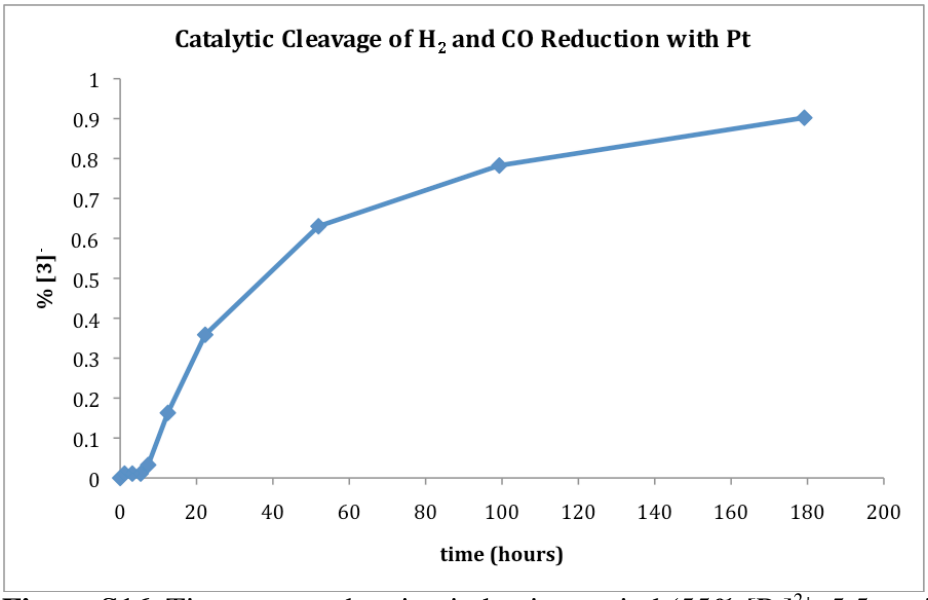

Figure S16. Time course showing induction period (55% $[Pt]^{2+}$, 5.5 equiv P_1, ~90% yield by integration to BAr^F_4 peaks).

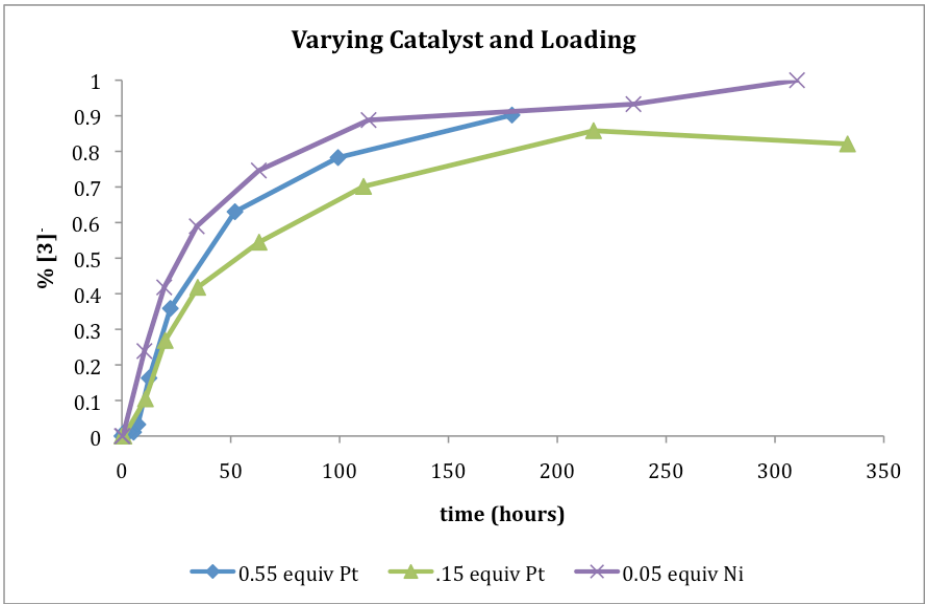

Figure S17. Time course of formation of [**3**]$^-$ under various catalysts and loading conditions, showing no major change in overall rates. Between 4 and 5.5 equiv phosphazene base were used in each case (non-pseudo first order).

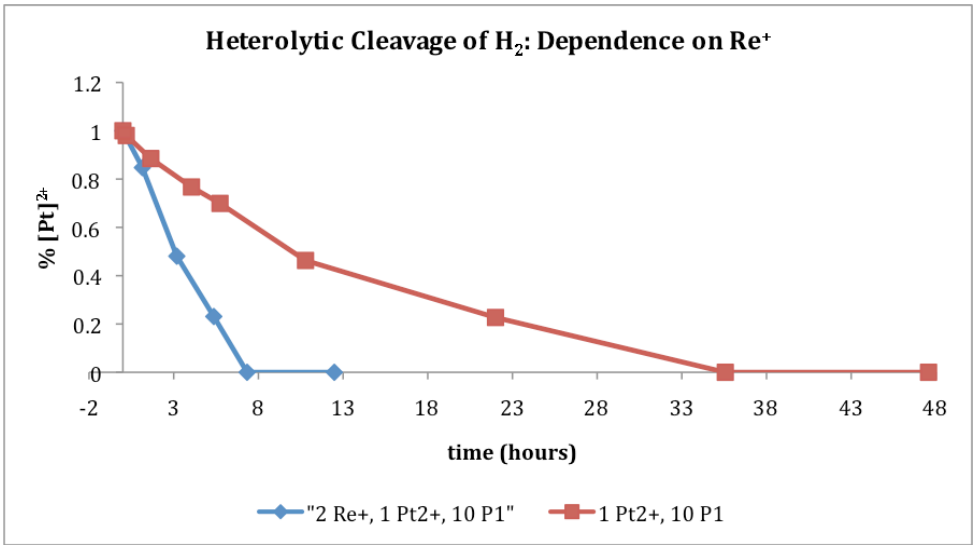

Figure S18. Comparison of formation of [**HPt**]$^+$ in presence and absence of [**1**]$^+$ (blue, 0.55 equiv [**Pt**]$^{2+}$, 5.5 equiv $\mathbf{P_1}$, 1 equiv [**1**]$^+$; red, 1 equiv [**Pt**]$^{2+}$, 10 equiv $\mathbf{P_1}$, no [**1**]$^+$).

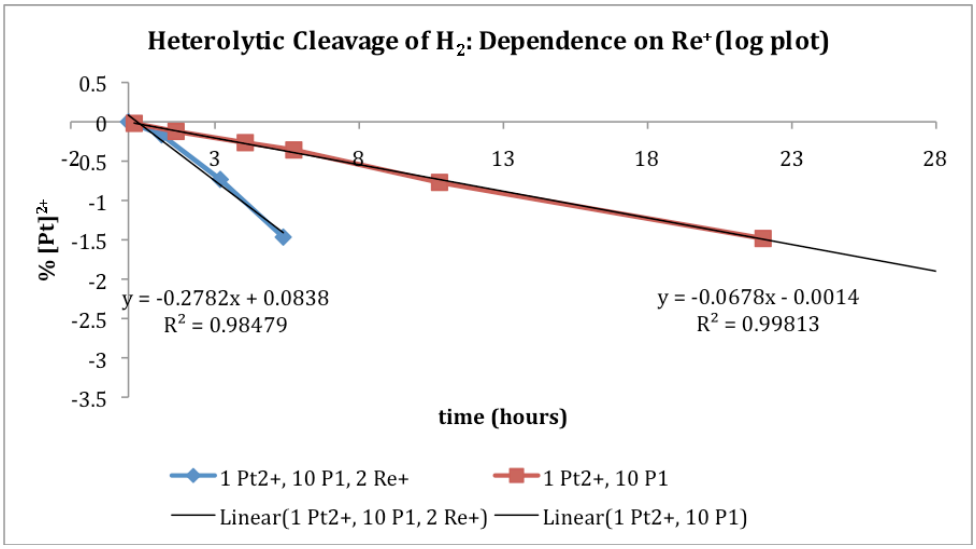

Figure S19. Log plot comparison of formation of [**HPt**]$^+$ in presence and absence of [**1**]$^+$ (blue, 0.55 equiv [**Pt**]$^{2+}$, 5.5 equiv $\mathbf{P_1}$, 1 equiv [**1**]$^+$; red, 1 equiv [**Pt**]$^{2+}$, 10 equiv $\mathbf{P_1}$, no [**1**]$^+$)

Reaction of [1][BAr$^F_4$] with [HPt][BAr$^F_4$].
In a glovebox, a vial was charged with [**1**][BAr$^F_4$] (36.3 mg, 0.020 mmol) and [**HPt**][BAr$^F_4$] (27.0 mg, 0.020 mmol). To the vial was added ~0.6 mL C_6D_5Cl, which dissolved the solids, and the reaction mixture was transferred to a J-Young NMR tube. Periodic NMR spectra were acquired, which showed no discernable reaction over more than 24 hours.

Reaction of [1][BF$_4$] with [HNi(dmpe)$_2$][PF$_6$].
A J-Young NMR tube was charged with 21.6 mg (0.021 mmol) [**1**][BF$_4$], 20.7 mg (0.041 mmol) [HNi(dmpe)$_2$][PF$_6$], and ~0.6 mL THF-d_8. Over 48 hours no discernable reaction took place, with only the starting materials visible by NMR spectroscopy.

Reaction of 2 with [Pt][BAr$^F_4$]$_2$.
Carbene **2** was prepared in the usual manner by dropwise addition of $NaHBEt_3$ (24.9 μL of a 1.0 M in toluene solution) into a rapidly stirring C_6D_5Cl solution of [**1**][BF$_4$] (26.2 mg, 0.025 mmol). The mixture was transferred to an NMR tube, and NMR studies showed essentially quantitative formation of **2**. The tube was returned to the glovebox and 85 mg (0.037 mmol) [**Pt**][BAr$^F_4$]$_2$ was added. The tube was sealed and shaken vigorously. Subsequent NMR studies showed complete conversion to [**1**][BAr$^F_4$] and [**HPt**][BAr$^F_4$].

General Procedure for Metal-Free H_2 Reductions.
In a glovebox, a J-Young NMR tube was charged with ~0.03 mmol [**1**][X] (X = BF$_4$ or BAr$^F_4$), ~0.06-0.60 mmol (2-20 equiv) $\mathbf{P_1}$, and ~0.6 mL THF-d_8. The tube was sealed, and NMR spectra (^{1}H, ^{31}P{^{1}H}) were obtained. The tube was degassed by two freeze-pump-thaw cycles, and between 1 and 4 atm H_2 was added by introducing H_2 at either 298 or 77 K. The tube was affixed to a slowly spinning motor to ensure good mixing, and the

reaction was monitored periodically by ^{1}H and ^{31}P NMR. When D_2 was used instead of H_2, all ^{1}H and ^{31}P signals were observed *except for the CH_2 group* of $[\mathbf{3}]^-$, verifying deuterium incorporation at that positions and confirming that dihydrogen is the sole source of hydride. Precise yields were measured by integration to a solution of $P(Mes)_3$ (Mes = 2,4,6-trimethylphenyl) in THF-d_8 in the J-Young tube in a coaxial capillary. Conditions: ~4 mM [**1**][BF_4], 10 equiv. P_1, ~3 atm H_2 (or D_2), giving yields of 92% for both H_2 and D_2. Integration to the protons of [BAr^F_4] gave similar yields (85-90%), except when 20 equiv P1 was added, when a reduced (70%) yield was obtained.

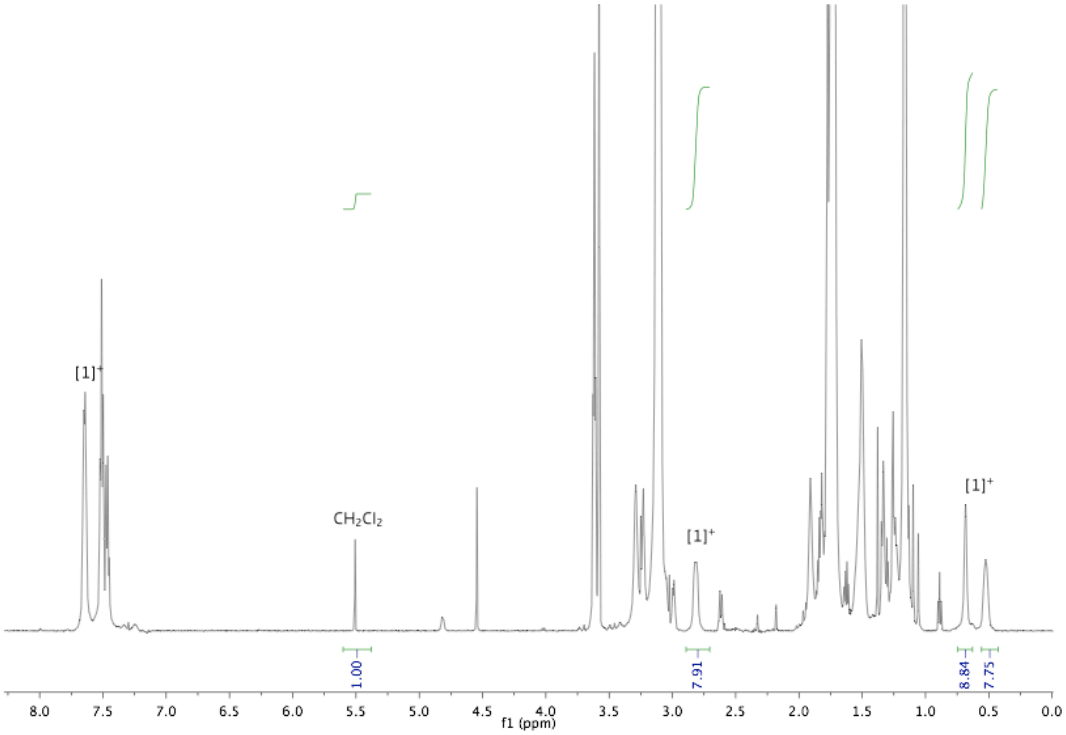

Figure S20. ^{1}H NMR immediately after H_2 addition (10 equiv $\mathbf{P_1}$). Minor CH_2Cl_2 impurity remains unchanged throughout the reaction; large peaks are $\mathbf{P_1}$, left off-scale to show the Re-containing species.

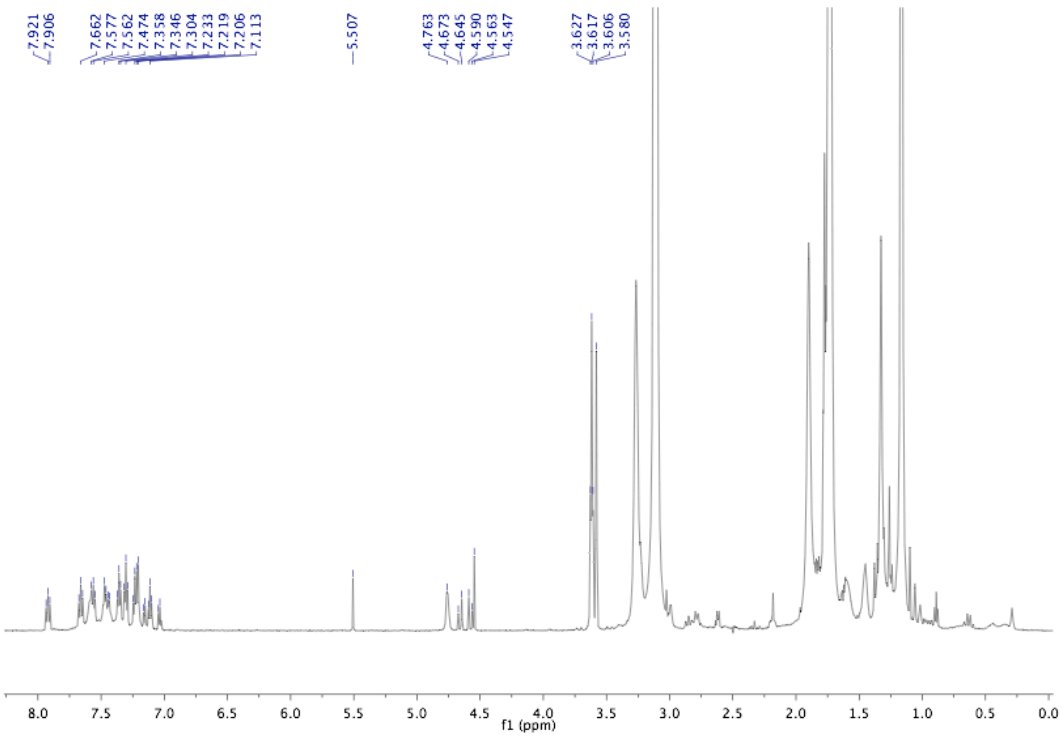

Figure S21. ^{1}H NMR after ~5 days (~85% yield).

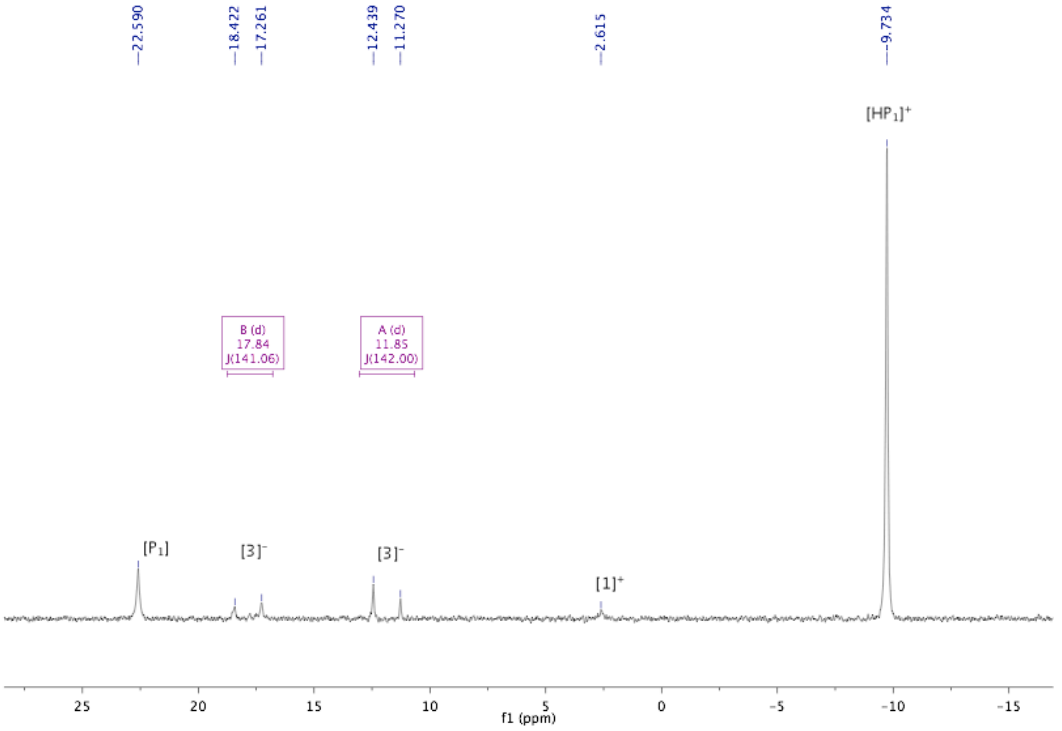

Figure S22. ^{31}P{^{1}H} NMR after ~5 days.

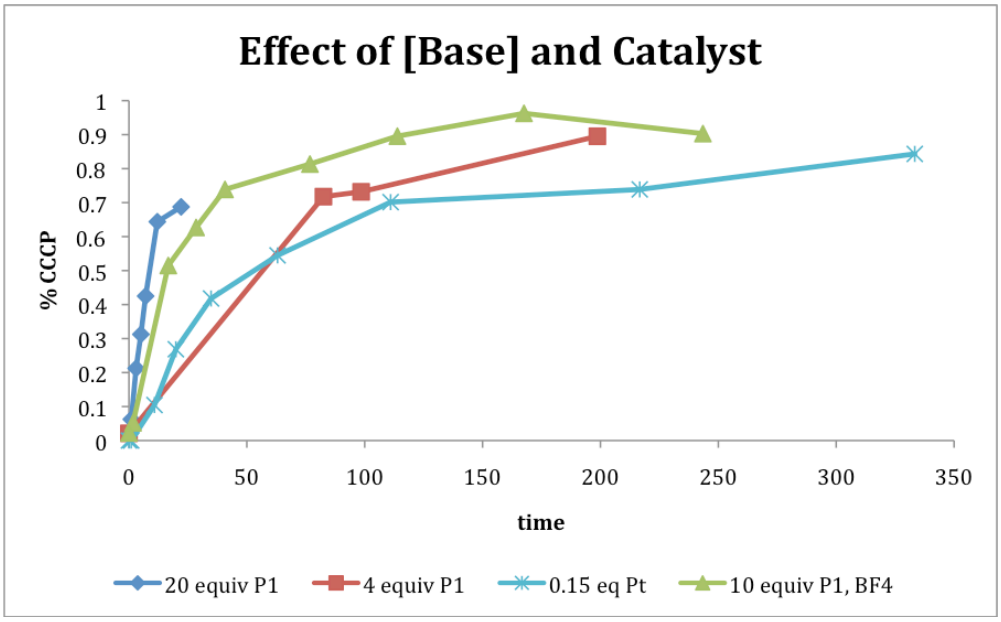

Figure S23. Crude comparison of rates of formation of [**3**]$^{-}$ with and without [**Pt**]$^{2+}$, and varying $\mathbf{P_1}$.

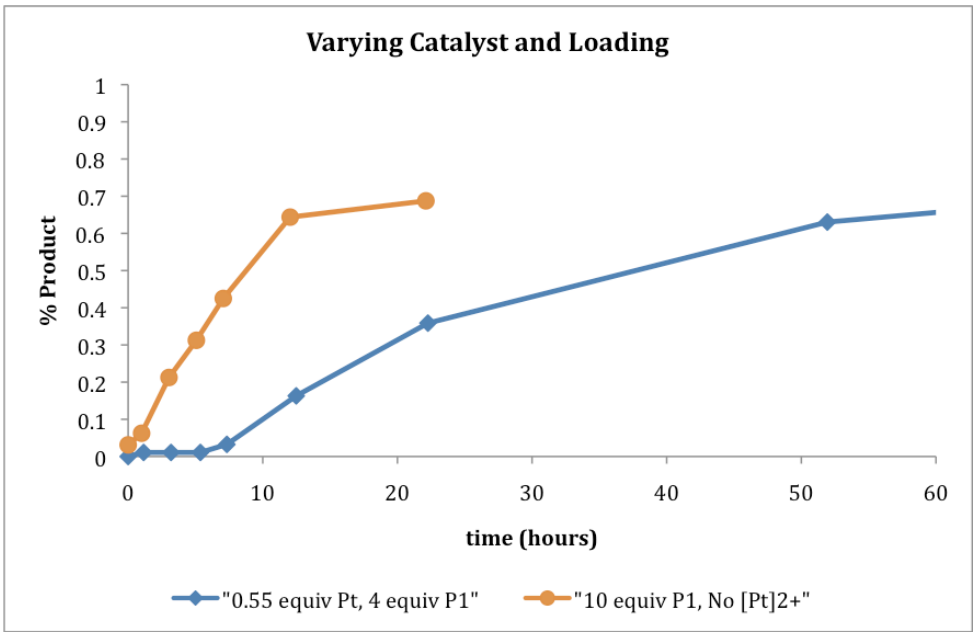

Figure S24. Time course clearly showing the elimination of induction period when [**Pt**]$^{2+}$ is omitted from the reaction.

NMR scale reaction of [1][BF_4] with H_2.

A J-Young Teflon-sealed NMR tube was charged with 12.2 mg (0.012 mmol) [**1**][BF_4] and ~0.6 mL THF-d_8. The tube was submerged in liquid nitrogen, and the headspace was evacuated, and refilled with H_2, affording ~2-3 atm H_2. The tube was sealed and the reaction monitored by ^{1}H and ^{31}P NMR. No reaction was discernable over a number of days.

H_2/D_2 Equilibration Experiments.
A J-Young Teflon-sealed NMR tube was charged with ~30 mg (0.1 mmol) **P_1** and 0.6 mL THF-d_8. After two freeze-pump-thaw cycles a 1:1 mixture of H_2:D_2, freshly mixed in a 500 mL bulb, was introduced while the tube was cooled to 77 K. The tube was sealed and the solution carefully thawed, and the reaction monitored by NMR. No HD peak was observed after 24 hours.
In a typical experiment, a J-Young NMR tube was charged with 31.2 mg (0.10 mmol) **P_1**, 20.6 mg (0.10 mmol) ^{t}BuCH$_2$CH$_2$B(C$_8$H$_{14}$), and ~0.6 mL THF-d_8. The tube was sealed and moved from the glovebox to a vacuum line, where it was subjected to two freeze-pump-thaw cycles, at which point a 1:1 H_2:D_2 mixture (freshly mixed in a 500 mL bulb) was introduced at 77 K. After carefully thawing the reaction mixture, the reaction was monitored by ^{1}H NMR. After 30 minutes a significant amount of HD (HD:H_2 was observed, which slowly increased. After two days, the ratio of HD:H_2 was 0.46:1.00. Another spectrum was taken 10 days later, showing complete equilibration (HD:H_2, 1.98:1.00) occurred at some point between 2 and 12 days from the start of the reaction.

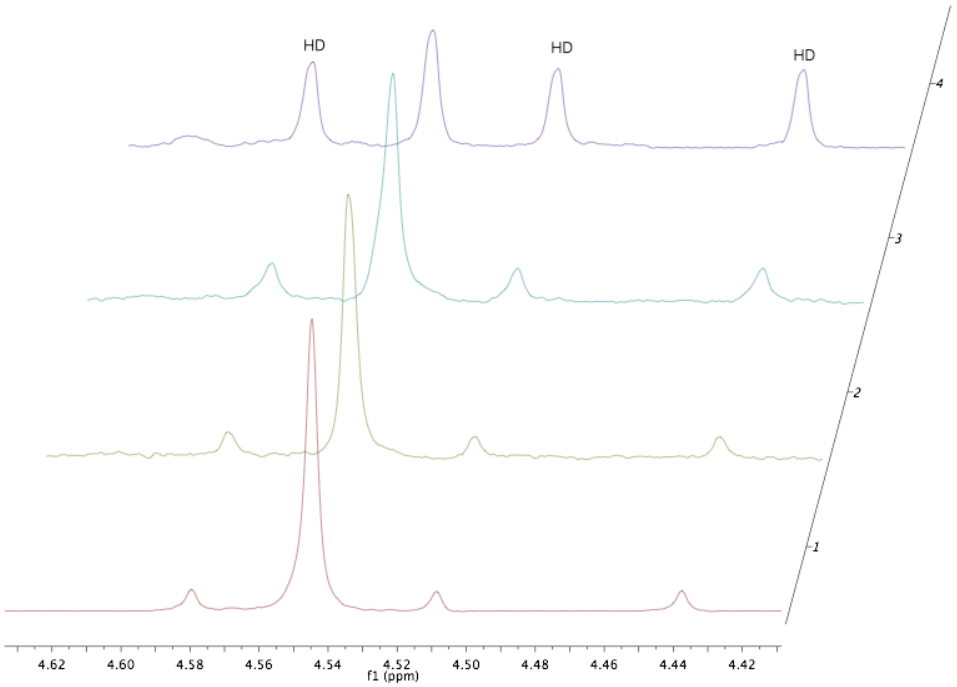

Figure S25. ^{1}H NMR of H_2/D_2 comproportionation to HD, monitored at 30 minutes, 24 hours, 2 days, 12 days.

Reaction of [(PPh$_3$)$_2$Re(CO)$_4$][BAr$^F_4$] with P_1 under H_2.
A J-Young NMR tube was charged with 40.6 mg (0.024 mmol) [(PPh$_3$)$_2$Re(CO)$_4$][BAr$^F_4$], and a ~0.6 mL THF-d_8 solution of 75 mg (0.24 mmol, 10 equiv) **P_1**. Before addition of H_2, initial NMR spectra were acquired, which showed a small amount of Re-H species (~7%), attributed to adventitious water (which could lead to hydroxide attack at Re-CO and elimination of CO_2 to give Re-H). The tube was freeze-pump-thawed twice, and H_2 was introduced at 77K (2-4 atm). The tube was affixed to a slowly spinning motor to

ensure good mixing, and the reaction monitored periodically by NMR spectroscopy. The amount of Re-H species remained essentially constant over more than 48 hours.

Reaction of $[(PPh_3)_2Re(CO)_4][BAr^F{}_4]$ with the frustrated Lewis pair P_1 / $^tBuCH_2CH_2B(C_8H_{14})$ under H_2.

A J-Young NMR tube was charged with 41.8 mg (0.025 mmol) $[(PPh_3)_2Re(CO)_4][BAr^F{}_4]$, and a ~0.6 mL THF-$d_8$ solution of 78 mg (0.25 mmol, 10 equiv) **P_1** and 5.1 mg (0.025 mmol, 1 equiv) $^tBuCH_2CH_2B(C_8H_{14})$. As in the absence of Lewis acid, a small amount (~2%) of Re-H species was initially formed, as above. The tube was freeze-pump-thawed twice, and H_2 was introduced at 77K (2-4 atm). After careful thawing, the tube was slowly rotated on a motor to mix, and was monitored by NMR spectroscopy. After a few hours, ~8% formyl was present; after 24 hours ~70% conversion to a mixture of Re formyl and hydride species was observed (formyl:hydride, 1.0:0.67), and after 48 hours ~80% conversion to the mixture of $(PPh_3)_2Re(CO)_3(CHO)$, $(PPh_3)_2Re(CO)_3H$, and $(PPh_3)Re(CO)_4H$ was observed (formyl: hydride, 1.0:1.37). After 48 hours all Re starting material had been consumed, and the other 20% Re comprised a few minor uncharacterized products.

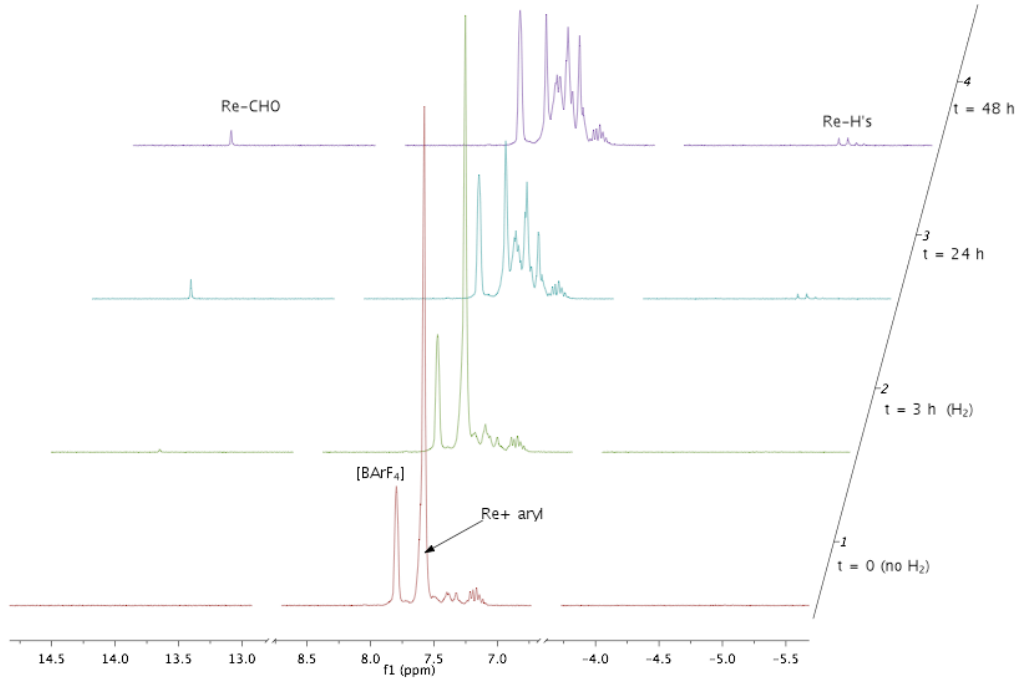

Figure S26. Time course (^{1}H NMR) of reduction facilitated by external Lewis acid. The single resonance for PPh_3 aromatic protons decreases as more complex aromatic signals grow in along with corresponding formyl and hydride resonances.

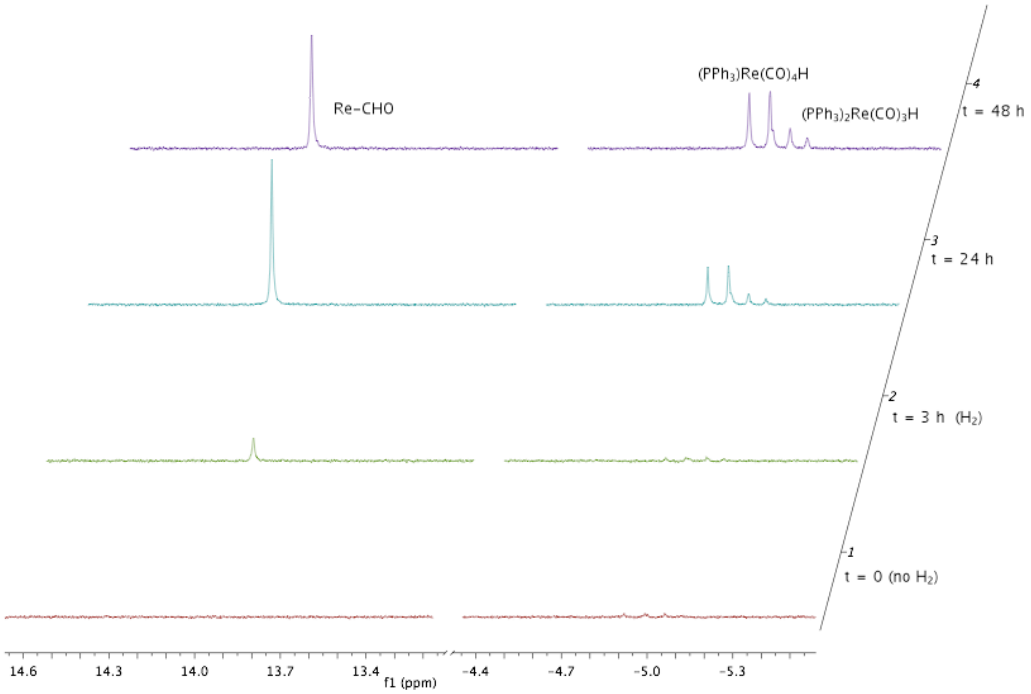

Figure S27. Blow-up showing Re-formyl and Re-H region over time. One peak of the triplet overlaps with the doublet.

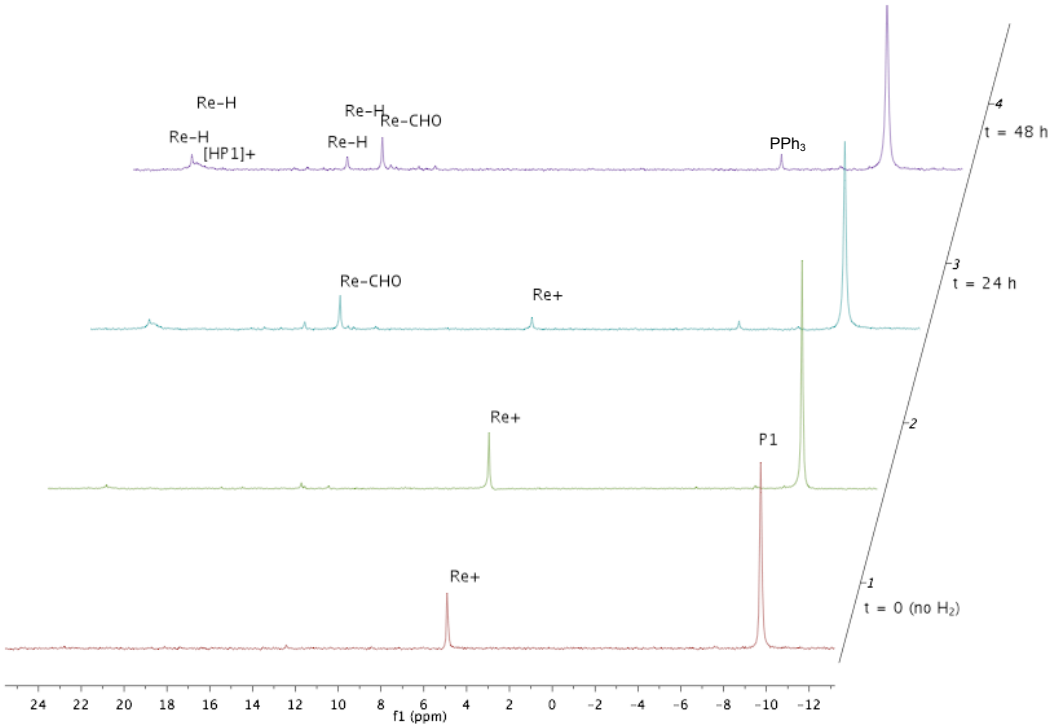

Figure S28. Time course (^{31}P NMR) of reduction facilitated by external Lewis acid.

II. Crystallographic Details.

Table 1. Crystal data and structure refinement for [1•(THF)$_2$][BF$_4$] (AJMM49) (CCDC 759590).

Empirical formula	$C_{56}H_{72}B_3F_4O_6P_2Re$
Formula weight	1197.71
Crystallization Solvent	THF/pentane
Crystal Habit	Block
Crystal size	0.27 x 0.26 x 0.19 mm^3
Crystal color	Colorless

Data Collection

Type of diffractometer	Bruker KAPPA APEX II	
Wavelength	0.71073 Å MoKα	
Data Collection Temperature	100(2) K	
θ range for 9538 reflections used in lattice determination	2.25 to 46.10°	
Unit cell dimensions	a = 9.7744(4) Å b = 10.3565(4) Å c = 14.9063(6) Å	α= 92.554(2)° β= 104.359(2)° γ = 105.481(2)°
Volume	1398.82(10) Å^3	
Z	1	
Crystal system	Triclinic	
Space group	P-1	
Density (calculated)	1.422 Mg/m^3	
F(000)	612	
Data collection program	Bruker APEX2 v2009.7-0	
θ range for data collection	2.25 to 49.35°	
Completeness to θ = 49.35°	98.4 %	
Index ranges	$-20 \le h \le 20$, $-21 \le k \le 22$, $-31 \le l \le 31$	
Data collection scan type	ω scans; 23 settings	
Data reduction program	Bruker SAINT-Plus v7.66A	
Reflections collected	108791	
Independent reflections	28016 [R_{int}= 0.0288]	
Absorption coefficient	2.290 mm^{-1}	
Absorption correction	Semi-empirical from equivalents	
Max. and min. transmission	0.7497 and 0.6272	

Table 1 (cont.)

Structure solution and Refinement

Structure solution program	SHELXS-97 (Sheldrick, 2008)
Primary solution method	Direct methods
Secondary solution method	Difference Fourier map
Hydrogen placement	Geometric positions
Structure refinement program	SHELXL-97 (Sheldrick, 2008)
Refinement method	Full matrix least-squares on F^2
Data / restraints / parameters	28016 / 0 / 349
Treatment of hydrogen atoms	Riding
Goodness-of-fit on F^2	2.373
Final R indices [$I>2\sigma(I)$, 27766 reflections]	R1 = 0.0306, *w*R2 = 0.0591
R indices (all data)	R1 = 0.0311, *w*R2 = 0.0592
Type of weighting scheme used	Sigma
Weighting scheme used	$w=1/\sigma^2(Fo^2)$
Max shift/error	0.001
Average shift/error	0.000
Largest diff. peak and hole	4.186 and -2.302 e.Å^{-3}

Special Refinement Details

Crystals were mounted on a glass fiber using Paratone oil then placed on the diffractometer under a nitrogen stream at 100K.

The tetrafluoroborate anion is disordered about a center of symmetry and is modeled with no restraints. The Re atom sits at a center of symmetry.

Refinement of F^2 against ALL reflections. The weighted R-factor (*w*R) and goodness of fit (S) are based on F^2, conventional R-factors (R) are based on F, with F set to zero for negative F^2. The threshold expression of $F^2 > 2\sigma(F^2)$ is used only for calculating R-factors(gt) etc. and is not relevant to the choice of reflections for refinement. R-factors based on F^2 are statistically about twice as large as those based on F, and R-factors based on ALL data will be even larger.

All esds (except the esd in the dihedral angle between two l.s. planes) are estimated using the full covariance matrix. The cell esds are taken into account individually in the estimation of esds in distances, angles and torsion angles; correlations between esds in cell parameters are only used when they are defined by crystal symmetry. An approximate (isotropic) treatment of cell esds is used for estimating esds involving l.s. planes.

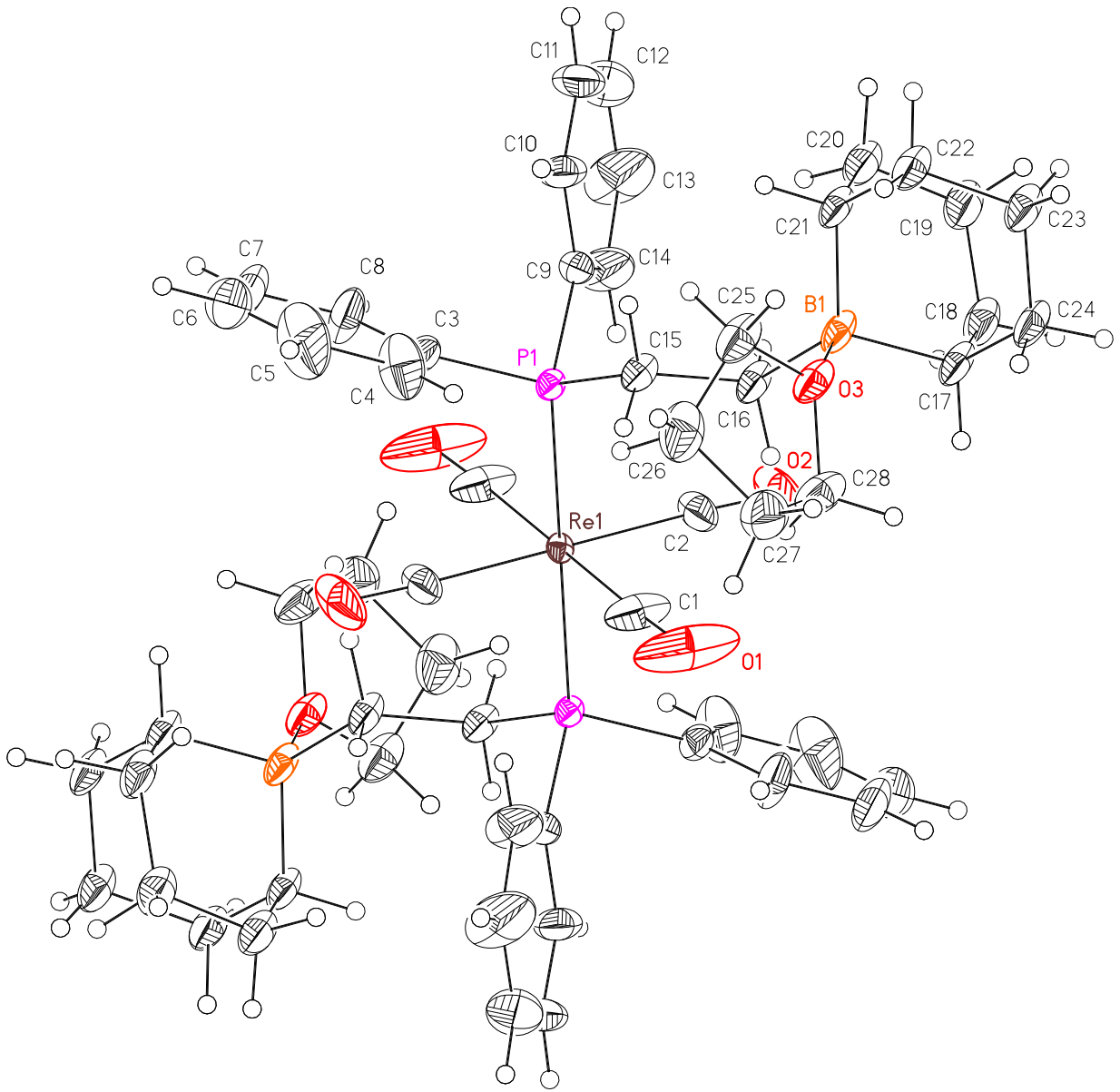
C11
C12
C10
C13
C20
C22
C21
C19
C23
C7
C8
C9
C14
C6
C3
C25
B1
C18
C24
C5
P1
C15
C4
03
C17
C16
C26
02
C28
Re1
C2
C27
C1
01

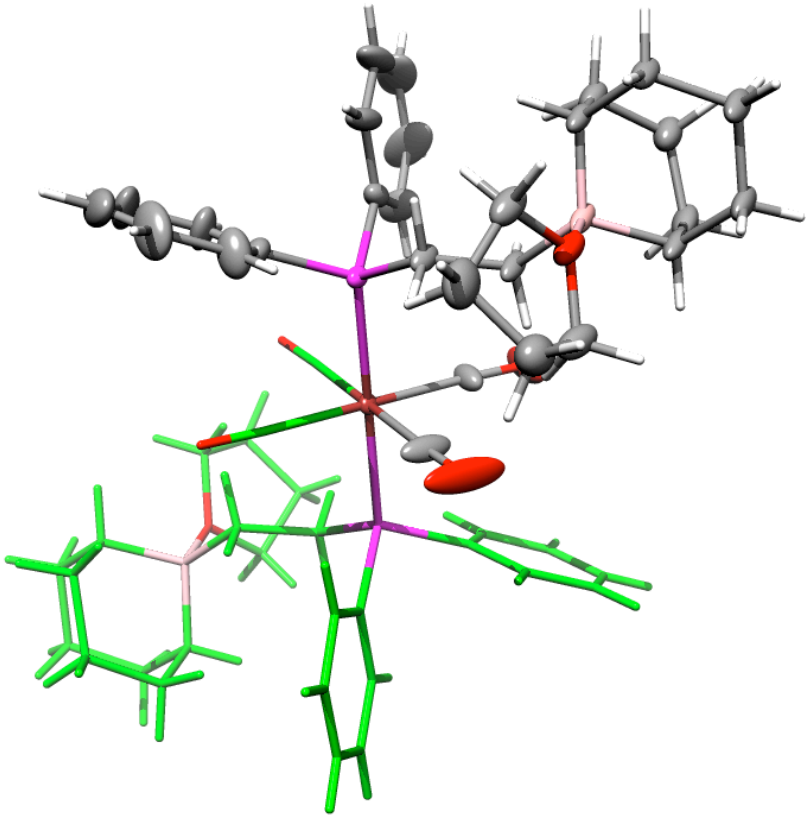

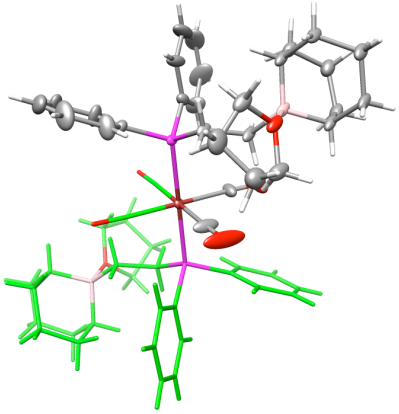

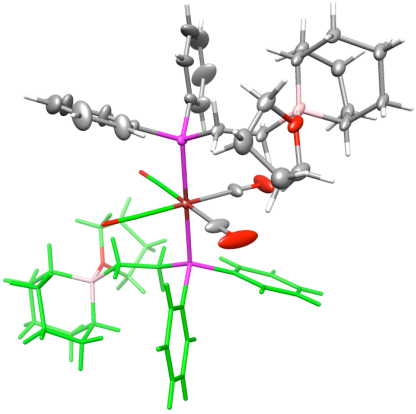

Table 2. Atomic coordinates (x 10^4) and equivalent isotropic displacement parameters ($Å^2$x 10^3) for [1•$(THF)_2$][BF_4] (AJMM49) (CCDC 759590). U(eq) is defined as the trace of the orthogonalized U^{ij} tensor.

	x	y	z	U_{eq}
Re(1)	5000	5000	5000	13(1)
P(1)	5234(1)	5965(1)	3568(1)	16(1)
O(1)	6268(3)	2696(2)	4500(1)	104(1)
O(2)	1977(2)	2936(2)	3964(1)	80(1)
O(3)	5825(1)	2594(1)	1400(1)	33(1)
B(1)	4152(2)	2772(1)	1366(1)	30(1)
C(1)	5863(2)	3567(2)	4688(1)	45(1)
C(2)	3049(2)	3719(2)	4344(1)	39(1)
C(3)	6713(1)	7536(1)	3723(1)	24(1)
C(4)	8039(2)	7563(2)	3540(1)	49(1)
C(5)	9140(2)	8784(3)	3654(2)	70(1)
C(6)	8929(2)	9963(2)	3955(2)	62(1)
C(7)	7643(2)	9945(2)	4146(2)	59(1)
C(8)	6519(2)	8735(1)	4027(1)	43(1)
C(9)	3681(1)	6478(1)	2901(1)	27(1)
C(10)	3824(2)	7153(1)	2124(1)	43(1)
C(11)	2671(3)	7590(2)	1618(1)	63(1)
C(12)	1402(3)	7403(2)	1881(2)	79(1)
C(13)	1255(2)	6749(3)	2632(3)	84(1)
C(14)	2381(2)	6273(2)	3151(2)	50(1)
C(15)	5560(1)	4868(1)	2699(1)	25(1)
C(16)	4300(2)	3546(1)	2373(1)	30(1)
C(17)	3042(2)	1260(1)	1156(1)	34(1)
C(18)	1497(2)	1378(1)	1146(1)	38(1)
C(19)	934(2)	2314(1)	459(1)	40(1)
C(20)	2098(2)	3651(1)	439(1)	36(1)
C(21)	3655(2)	3537(1)	473(1)	31(1)
C(22)	3698(2)	2794(1)	-437(1)	36(1)
C(23)	2852(2)	1283(1)	-620(1)	41(1)
C(24)	3088(2)	523(1)	245(1)	39(1)
C(25)	7013(2)	3608(1)	1165(1)	38(1)
C(26)	8428(2)	3638(2)	1909(1)	49(1)
C(27)	8097(2)	2189(2)	2134(1)	47(1)
C(28)	6472(2)	1819(1)	2106(1)	41(1)
B(2)	9772(3)	4397(4)	4887(3)	36(1)
F(1)	8569(3)	4842(3)	4623(3)	80(1)
F(2)	9290(4)	3035(3)	4893(4)	121(2)
F(3)	10636(4)	4693(6)	4351(4)	145(2)
F(4)	10567(5)	4993(3)	5779(2)	93(1)

Table 3. Selected bond lengths [Å] and angles [°] for [1•$(THF)_2$][BF_4] (AJMM49) (CCDC 759590).

Re(1)-C(1)	1.9832(13)	C(1)-Re(1)-C(1)#1	179.999(1)
Re(1)-C(1)#1	1.9832(13)	C(1)-Re(1)-C(2)#1	93.65(9)
Re(1)-C(2)#1	1.9902(11)	C(1)#1-Re(1)-C(2)#1	86.35(9)
Re(1)-C(2)	1.9903(11)	C(1)-Re(1)-C(2)	86.35(9)
Re(1)-P(1)#1	2.4324(2)	C(1)#1-Re(1)-C(2)	93.65(9)
Re(1)-P(1)	2.4324(2)	C(2)#1-Re(1)-C(2)	180.00(8)
		C(1)-Re(1)-P(1)#1	89.04(3)
		C(1)#1-Re(1)-P(1)#1	90.96(3)
		C(2)#1-Re(1)-P(1)#1	91.43(3)
		C(2)-Re(1)-P(1)#1	88.57(3)
		C(1)-Re(1)-P(1)	90.96(3)
		C(1)#1-Re(1)-P(1)	89.04(3)
		C(2)#1-Re(1)-P(1)	88.57(3)
		C(2)-Re(1)-P(1)	91.43(3)
		P(1)#1-Re(1)-P(1)	180.0

Symmetry transformations used to generate equivalent atoms:
#1 -x+1,-y+1,-z+1

Table 4. Bond lengths [Å] and angles [°] for [1•(THF)$_2$][BF$_4$] (AJMM49) (CCDC 759590).

Re(1)-C(1)	1.9832(13)	F(1)-B(2)#2	1.569(4)
Re(1)-C(1)#1	1.9832(13)	F(3)-F(4)#2	1.273(7)
Re(1)-C(2)#1	1.9902(11)	F(3)-F(1)#2	1.523(6)
Re(1)-C(2)	1.9903(11)	F(3)-B(2)#2	1.634(5)
Re(1)-P(1)#1	2.4324(2)	F(4)-F(1)#2	1.134(5)
Re(1)-P(1)	2.4324(2)	F(4)-B(2)#2	1.225(5)
P(1)-C(9)	1.8180(12)	F(4)-F(3)#2	1.273(7)
P(1)-C(3)	1.8267(10)		
P(1)-C(15)	1.8272(9)	C(1)-Re(1)-C(1)#1	179.999(1)
O(1)-C(1)	1.1270(18)	C(1)-Re(1)-C(2)#1	93.65(9)
O(2)-C(2)	1.1348(16)	C(1)#1-Re(1)-C(2)#1	86.35(9)
O(3)-C(25)	1.4689(15)	C(1)-Re(1)-C(2)	86.35(9)
O(3)-C(28)	1.4725(18)	C(1)#1-Re(1)-C(2)	93.65(9)
O(3)-B(1)	1.683(2)	C(2)#1-Re(1)-C(2)	180.00(8)
B(1)-C(17)	1.6156(16)	C(1)-Re(1)-P(1)#1	89.04(3)
B(1)-C(21)	1.6171(17)	C(1)#1-Re(1)-P(1)#1	90.96(3)
B(1)-C(16)	1.6240(15)	C(2)#1-Re(1)-P(1)#1	91.43(3)
C(3)-C(8)	1.3788(19)	C(2)-Re(1)-P(1)#1	88.57(3)
C(3)-C(4)	1.3832(19)	C(1)-Re(1)-P(1)	90.96(3)
C(4)-C(5)	1.397(2)	C(1)#1-Re(1)-P(1)	89.04(3)
C(5)-C(6)	1.366(4)	C(2)#1-Re(1)-P(1)	88.57(3)
C(6)-C(7)	1.352(3)	C(2)-Re(1)-P(1)	91.43(3)
C(7)-C(8)	1.400(2)	P(1)#1-Re(1)-P(1)	180.0
C(9)-C(14)	1.377(2)	C(9)-P(1)-C(3)	100.32(5)
C(9)-C(10)	1.3956(17)	C(9)-P(1)-C(15)	102.77(6)
C(10)-C(11)	1.387(3)	C(3)-P(1)-C(15)	104.49(5)
C(11)-C(12)	1.360(4)	C(9)-P(1)-Re(1)	117.29(4)
C(12)-C(13)	1.351(4)	C(3)-P(1)-Re(1)	114.95(4)
C(13)-C(14)	1.398(2)	C(15)-P(1)-Re(1)	115.03(3)
C(15)-C(16)	1.5397(16)	C(25)-O(3)-C(28)	109.26(13)
C(17)-C(18)	1.544(2)	C(25)-O(3)-B(1)	124.75(9)
C(17)-C(24)	1.5445(15)	C(28)-O(3)-B(1)	118.78(9)
C(18)-C(19)	1.544(2)	C(17)-B(1)-C(21)	106.61(11)
C(19)-C(20)	1.5467(17)	C(17)-B(1)-C(16)	113.80(8)
C(20)-C(21)	1.546(2)	C(21)-B(1)-C(16)	115.66(9)
C(21)-C(22)	1.5447(15)	C(17)-B(1)-O(3)	105.54(10)
C(22)-C(23)	1.5379(16)	C(21)-B(1)-O(3)	108.07(8)
C(23)-C(24)	1.5410(18)	C(16)-B(1)-O(3)	106.59(11)
C(25)-C(26)	1.534(3)	O(1)-C(1)-Re(1)	175.7(2)
C(26)-C(27)	1.519(2)	O(2)-C(2)-Re(1)	176.1(2)
C(27)-C(28)	1.520(3)	C(8)-C(3)-C(4)	118.41(12)
B(2)-B(2)#2	1.210(7)	C(8)-C(3)-P(1)	119.93(9)
B(2)-F(4)#2	1.225(5)	C(4)-C(3)-P(1)	121.66(11)
B(2)-F(3)	1.289(4)	C(3)-C(4)-C(5)	120.21(19)
B(2)-F(1)	1.352(4)	C(6)-C(5)-C(4)	120.61(19)
B(2)-F(2)	1.364(5)	C(7)-C(6)-C(5)	119.65(14)
B(2)-F(4)	1.383(5)	C(6)-C(7)-C(8)	120.69(18)
B(2)-F(1)#2	1.569(4)	C(3)-C(8)-C(7)	120.43(16)
B(2)-F(3)#2	1.634(5)	C(14)-C(9)-C(10)	118.36(13)
F(1)-F(4)#2	1.134(5)	C(14)-C(9)-P(1)	122.58(10)
F(1)-F(3)#2	1.523(6)	C(10)-C(9)-P(1)	119.02(12)

C(11)-C(10)-C(9)	120.24(19)	F(3)-B(2)-F(4)	107.7(3)
C(12)-C(11)-C(10)	120.90(18)	F(1)-B(2)-F(4)	108.9(4)
C(13)-C(12)-C(11)	119.19(18)	F(2)-B(2)-F(4)	109.1(4)
C(12)-C(13)-C(14)	121.6(2)	B(2)#2-B(2)-F(1)#2	56.4(3)
C(9)-C(14)-C(13)	119.65(19)	F(4)#2-B(2)-F(1)#2	104.9(3)
C(16)-C(15)-P(1)	112.43(7)	F(3)-B(2)-F(1)#2	63.5(3)
C(15)-C(16)-B(1)	116.16(8)	F(1)-B(2)-F(1)#2	131.7(3)
C(18)-C(17)-C(24)	113.54(13)	F(2)-B(2)-F(1)#2	118.8(3)
C(18)-C(17)-B(1)	107.13(10)	F(4)-B(2)-F(1)#2	44.6(2)
C(24)-C(17)-B(1)	111.21(9)	B(2)#2-B(2)-F(3)#2	51.3(3)
C(19)-C(18)-C(17)	114.65(10)	F(4)#2-B(2)-F(3)#2	97.0(4)
C(18)-C(19)-C(20)	114.90(14)	F(3)-B(2)-F(3)#2	132.9(3)
C(21)-C(20)-C(19)	115.60(12)	F(1)-B(2)-F(3)#2	60.5(3)
C(22)-C(21)-C(20)	112.34(12)	F(2)-B(2)-F(3)#2	115.5(4)
C(22)-C(21)-B(1)	111.60(10)	F(4)-B(2)-F(3)#2	49.1(3)
C(20)-C(21)-B(1)	107.16(9)	F(1)#2-B(2)-F(3)#2	86.7(3)
C(23)-C(22)-C(21)	115.11(8)	F(4)#2-F(1)-B(2)	58.3(3)
C(22)-C(23)-C(24)	114.20(11)	F(4)#2-F(1)-F(3)#2	107.8(3)
C(23)-C(24)-C(17)	115.48(10)	B(2)-F(1)-F(3)#2	69.0(3)
O(3)-C(25)-C(26)	105.54(12)	F(4)#2-F(1)-B(2)#2	59.0(2)
C(27)-C(26)-C(25)	101.93(14)	B(2)-F(1)-B(2)#2	48.3(3)
C(26)-C(27)-C(28)	103.45(15)	F(3)#2-F(1)-B(2)#2	49.3(2)
O(3)-C(28)-C(27)	105.02(11)	F(4)#2-F(3)-B(2)	57.1(2)
B(2)#2-B(2)-F(4)#2	69.2(4)	F(4)#2-F(3)-F(1)#2	105.1(3)
B(2)#2-B(2)-F(3)	81.6(4)	B(2)-F(3)-F(1)#2	67.2(3)
F(4)#2-B(2)-F(3)	60.8(4)	F(4)#2-F(3)-B(2)#2	55.1(2)
B(2)#2-B(2)-F(1)	75.3(3)	B(2)-F(3)-B(2)#2	47.1(3)
F(4)#2-B(2)-F(1)	51.9(3)	F(1)#2-F(3)-B(2)#2	50.5(2)
F(3)-B(2)-F(1)	112.7(4)	F(1)#2-F(4)-B(2)#2	69.8(3)
B(2)#2-B(2)-F(2)	163.8(6)	F(1)#2-F(4)-F(3)#2	131.9(4)
F(4)#2-B(2)-F(2)	125.4(4)	B(2)#2-F(4)-F(3)#2	62.1(4)
F(3)-B(2)-F(2)	110.9(5)	F(1)#2-F(4)-B(2)	76.4(3)
F(1)-B(2)-F(2)	107.5(3)	B(2)#2-F(4)-B(2)	54.9(3)
B(2)#2-B(2)-F(4)	55.9(3)	F(3)#2-F(4)-B(2)	75.8(3)
F(4)#2-B(2)-F(4)	125.1(3)		

Symmetry transformations used to generate equivalent atoms:
#1 -x+1,-y+1,-z+1 #2 -x+2,-y+1,-z+1

Table 5. Anisotropic displacement parameters ($Å^2$x 10^4) for [1•$(THF)_2$][BF_4] (AJMM49) (CCDC 759590). The anisotropic displacement factor exponent takes the form: $-2\pi^2$[$h^2a^{*2}U^{11}$ + ... + 2 h k a* b* U^{12}]

	U^{11}	U^{22}	U^{33}	U^{23}	U^{13}	U^{12}
Re(1)	154(1)	137(1)	114(1)	-7(1)	56(1)	32(1)
P(1)	226(1)	132(1)	135(1)	4(1)	76(1)	49(1)
O(1)	2300(30)	1126(14)	590(10)	482(10)	875(15)	1459(19)
O(2)	574(8)	830(10)	430(7)	246(7)	-162(5)	-489(8)
O(3)	617(6)	173(3)	256(4)	39(2)	246(4)	91(3)
B(1)	594(8)	127(4)	205(4)	12(3)	229(5)	47(4)
C(1)	890(12)	489(7)	289(6)	190(5)	365(7)	505(8)
C(2)	319(5)	418(7)	241(5)	119(4)	-17(4)	-144(5)
C(3)	279(4)	187(4)	239(4)	51(3)	85(3)	21(3)
C(4)	301(6)	544(9)	548(10)	-88(7)	197(6)	-46(6)
C(5)	380(8)	811(15)	714(14)	-40(11)	236(9)	-211(9)
C(6)	460(9)	473(9)	615(11)	214(8)	-45(8)	-209(7)
C(7)	525(9)	186(5)	843(14)	81(6)	-79(9)	2(5)
C(8)	360(6)	175(5)	696(11)	-10(5)	96(6)	35(4)
C(9)	346(5)	208(4)	207(4)	8(3)	-13(3)	99(3)
C(10)	800(11)	307(6)	197(5)	55(4)	49(5)	277(6)
C(11)	1078(18)	383(8)	324(7)	36(6)	-176(9)	359(9)
C(12)	653(13)	532(11)	908(18)	165(11)	-366(12)	221(9)
C(13)	300(7)	695(13)	1410(30)	486(16)	-60(11)	161(8)
C(14)	235(5)	513(9)	718(12)	283(8)	16(6)	109(5)
C(15)	431(5)	173(3)	190(4)	21(3)	184(4)	90(3)
C(16)	593(7)	143(3)	202(4)	9(3)	230(5)	45(4)
C(17)	674(8)	131(3)	225(4)	20(3)	239(5)	26(4)
C(18)	625(8)	197(4)	289(5)	21(4)	228(6)	-27(5)
C(19)	584(8)	250(5)	325(6)	18(4)	189(6)	7(5)
C(20)	606(8)	192(4)	292(5)	35(3)	202(5)	54(5)
C(21)	591(7)	133(3)	210(4)	21(3)	211(5)	35(4)
C(22)	718(9)	181(4)	207(4)	25(3)	244(5)	47(5)
C(23)	809(10)	181(4)	225(5)	-10(3)	251(6)	39(5)
C(24)	782(10)	132(4)	253(5)	0(3)	247(6)	46(5)
C(25)	624(9)	240(5)	368(6)	55(4)	309(6)	103(5)
C(26)	628(10)	367(7)	474(9)	-73(6)	242(8)	82(7)
C(27)	643(10)	376(7)	394(8)	24(6)	127(7)	145(7)
C(28)	753(10)	269(5)	342(6)	93(4)	291(7)	220(6)
B(2)	260(11)	402(14)	449(17)	50(12)	109(11)	110(10)
F(1)	382(11)	649(16)	1500(30)	269(19)	357(17)	262(11)
F(2)	770(20)	406(14)	1970(50)	140(20)	-390(20)	71(13)
F(3)	487(16)	2420(60)	1260(40)	-540(40)	610(20)	-110(30)
F(4)	1220(30)	708(19)	426(14)	107(12)	-115(16)	-137(19)

1. Pangborn, A. B.; Giardello, M. A.; Grubbs, R. H.; Rosen, R. K.; Timmers, F. J., *Organometallics* **1996,** *15*, 1518-20.
2. Miller, A. J. M.; Labinger, J. A.; Bercaw, J. E., *J. Am. Chem. Soc.* **2008,** *130*, 11874-11875.
3. Miedaner, A.; DuBois, D. L.; Curtis, C. J.; Haltiwanger, R. C., *Organometallics* **1993,** *12*, 299-303.
4. Berning, D. E.; Noll, B. C.; DuBois, D. L., *J. Am. Chem. Soc.* **1999,** *121*, 11432-11447.
5. Hirano, K.; Yorimitsu, H.; Oshima, K., *Organic Letters* **2005,** *7*, 4689-4691.
6. Curtis, C. J.; Miedaner, A.; Ellis, W. W.; DuBois, D. L., *J. Am. Chem. Soc.* **2002,** *124*, 1918-1925.
7. Benesi, H. A.; Hildebrand, J. H., *J. Am. Chem. Soc.* **1949,** *71*, 2703-2707.
8. Rose, N. J.; Drago, R. S., *J. Am. Chem. Soc.* **1959,** *81*, 6138-6141.
9. Baldwin, S. M.; Bercaw, J. E.; Brintzinger, H. H., *J. Am. Chem. Soc.* **2008,** *130*, 17423-17433.